DOKUZ EYLÜL UNIVERSITY
GRADUATE SCHOOL OF NATURAL AND APPLIED SCIENCES

SPECTRAL DOMAIN WAVEFORM DESIGN FOR MIMO RADAR SYSTEMS

by
Ozan KOZAKÇIOĞLU

June, 2018
İZMİR

SPECTRAL DOMAIN WAVEFORM DESIGN FOR MIMO RADAR SYSTEMS

A Thesis Submitted to the
Graduate School of Natural And Applied Sciences of Dokuz Eylül University
In Partial Fulfillment of the Requirements for the Degree of Master of Science in
Electrical and Electronics Engineering Program

by
Ozan KOZAKÇIOĞLU

June, 2018
İZMİR

M.Sc THESIS EXAMINATION RESULT FORM

We have read the thesis entitled "**SPECTRAL DOMAIN WAVEFORM DESIGN FOR MIMO RADAR SYSTEMS**" completed by **Ozan KOZAKÇIOĞLU** under supervision of **ASSOC. PROF. DR. OLCAY AKAY** and we certify that in our opinion it is fully adequate, in scope and in quality, as a thesis for the degree of Master of Science.

....

Assoc. Prof. Dr. Olcay AKAY

Supervisor

....

Instructor Dr. M. Emre ÇEK

Jury Member

....

Instructor Dr. Mümtaz YILMAZ

Jury Member

Prof. Dr. Latif SALUM

Director

Graduate School of Natural and Applied Sciences

ACKNOWLEDGEMENTS

I would like to express my deepest gratitude to the people who have helped and supported me throughout my project.

I am grateful to my advisor Assoc. Prof. Dr. Olcay AKAY for his continuous support during this project.

I wish to thank my parents for their undivided support and interest who inspired me and encouraged me to go my own way, without whom I would be unable to complete my project.

At last but not the least, I want to thank my friends who appreciated me for my work and motivated me and finally to God who made all the things possible.

Ozan KOZAKÇIOĞLU

SPECTRAL DOMAIN WAVEFORM DESIGN FOR MIMO RADAR SYSTEMS

ABSTRACT

In radar systems, interference between the transmit signal and communication signals possibly existing in the same spectrum band is a serious concern. As a possible solution to this problem, cognitive radars having transmit signals whose spectra contain notches are proposed. Two algorithms named SCAN and SHAPE can be used for designing such radar transmit signals with desirable spectral characteristics. The SCAN algorithm can also reduce sidelobes of the temporal autocorrelations of the designed sequences via some additional constraints.

In this thesis, we introduce generalizations of both SCAN and SHAPE algorithms for multiple-input multiple-output (MIMO) radar systems. SCAN and SHAPE are both iterative algorithms employing fast Fourier transform (FFT). Hence, they allow design of long sequences in an efficient manner. We also provide numerical simulation examples of MIMO SCAN and MIMO SHAPE algorithms comparing their performances against each other.

The proposed MIMO algorithms can be utilized for generating signals used in other application areas such as communications. As an example, to generate orthogonal frequency division multiplexing (OFDM) signals, the proposed methods can be exploited.

Keywords: Radar sequence design, frequency stopband suppression, MIMO radar systems

MIMO RADARLAR İÇİN SPEKTRUM BOYUTUNDA SİNYAL TASARIMI

ÖZ

Radar sistemlerinde, gönderim sinyali ile muhtemelen aynı spektrum bandında mevcut iletişim sinyalleri arasındaki girişim ciddi bir endişe kaynağıdır. Bu probleme olası bir çözüm olarak, tayfları çentikler içeren verici sinyallere sahip kognitif radarlar önerilmektedir. SCAN ve SHAPE adında iki algoritma istenilen spektral özelliklere sahip bu radar gönderim sinyallerinin tasarımı için kullanılabilir. SCAN algoritması, bazı ilave kısıtlamalar yoluyla tasarımı yapılan dizilerin zamansal otokorelasyonlarının yan çubuklarını da azaltabilir.

Bu tezde, çok girişli çoklu çıkış (MIMO) radar sistemleri için SCAN ve SHAPE algoritmalarının genellemeleri sunulmaktadır. SCAN ve SHAPE, hızlı Fourier dönüşümü (FFT) kullanan iteratif algoritmalardır. Dolayısıyla, uzun dizilerin verimli bir şekilde tasarımlanmasına izin verirler. MIMO SCAN ve MIMO SHAPE algoritmalarının performanslarını birbirleriyle karşılaştıran sayısal simülasyon örnekleri de sağlanmaktadır.

Önerilen MIMO algoritmaları, iletişim gibi diğer uygulama alanlarında kullanılan sinyalleri üretmek için de kullanılabilir. Örnek olarak, ortogonal frekans bölüşümlü çoğullama (OFDM) sinyallerinin üretilmesi için önerilen yöntemlerden faydalanmak mümkündür.

Anahtar kelimeler: Radar dizi tasarımı, frekans stopbant bastırımı, MIMO radar sistemleri

CONTENTS

Page

LIST OF FIGURES

Page

LIST OF TABLES

Page

CHAPTER ONE
INTRODUCTION

Recently, cognitive radar has drawn the attention of many researchers (Haykin, 2007). Put simply, cognitive radar can adapt itself to the changing dynamics of the environment. It can be employed when there is a possibility for the radar transmit signal to interfere with signals emanating from other sources such as local communication systems, navigation systems, or military communication systems whose operating frequency band might overlap with the spectral band of the radar transmit signal. This overlap could be prevented to a certain degree by designing radar transmit signals with spectral notches over the interfering frequency bands. There exist various works proposing design of such radar transmit signals with desirable spectral characteristics (Lindenfeld, 2004), (Wang & Lu, 2010), (Cook et al., 2010).

There are several types of sequences proposed in the literature employed as radar transmit signals. Sequences having a constant modulus of one and different phase values for all of its elements are called unimodular sequences. Unimodular sequences can be generated by methods which determine the phase values of the sequence elements using predetermined fixed formulas (Petrolati et al., 2012), (Levanon & Mozeson, 2004). On the other hand, another way of generating unimodular sequences is through some iterative numerical optimization algorithms which are started by a fixed initial sequence (Wang & Lu, 2010), (He et al., 2010), (Song et al., 2015).

Generally, only designing radar transmit sequences having unimodular characteristic might not fulfil all the requirements of a radar system. Depending on the application, the designed radar sequences need to be further improved to inherit some properties, for instance target detection capabilities and good Doppler resolution. Accordingly, several algorithms have been developed for enhancing certain properties of the designed radar sequences such as reducing correlation sidelobe levels in the temporal domain or suppressing some specified frequency bands in the spectral domain or both (Stoica et al., 2009), (He et al., 2010), (Rowe et al., 2014).

In communications, the idea of suppressing frequencies at some stopbands and thus forming a sequence is employed to generate orthogonal frequency division multiplexing (OFDM) signals having desirable power spectral density characteristics. OFDM signals are orthogonal to each other which means that mutual cross-correlations of those signals become approximately zero ensuring that they do not interfere with each other (Sebt et al., 2008).

Radar systems in which only one designed radar transmit sequence is employed are classified as single input single output (SISO) radar systems. On the other hand, using at least two radar sequences provides some advantages such as better correlation properties. Sytstems in which two or more sequences are designed and employed are called as multiple input and multiple output (MIMO) radar systems. By employing orthogonal radar transmit sequences, MIMO radars can accomplish greatly increased virtual aperture which provides better detection performance (Fishler et al., 2006), improved parameter identifiability (Li et al., 2007), enhanced resolution (Bliss & Forsythe, 2003) and direct applicability of array techniques (Xu et al., 2008).

In this thesis, we first review two existing techniques that are named as SCAN (stopband cyclic algorithm-new) (He et al., 2010) and SHAPE (Rowe et al., 2014) algorithms which have been proposed for designing radar transmit signals with some spectral domain constraints. Differing from the SHAPE algorithm, the SCAN algorithm also aims at reducing sidelobe levels of the temporal autocorrelation of the designed sequence via some additional constraints. Then, we propose extensions of SCAN and SHAPE for MIMO radar systems and present some simulation examples.

The rest of the thesis is organized as follows: An overview of SCAN and SHAPE algorithms is presented in Chapter Two. Extensions of both algorithms for MIMO radar systems are proposed in Chapter Three. Numerical examples of the proposed MIMO SCAN and MIMO SHAPE algorithms are given in Chapter Four. Comparison of the proposed algorithms in term of certain performance metrics is carried out in Chapter Four, as well. Finally, we end up with some concluding remarks in Chapter

Five.

Notation: Boldface lowercase letters denote vectors while boldface uppercase letters denote matrices. $[\cdot]^H$ and $[\cdot]^T$ represent Hermitian and transpose operations, respectively, and $\|\cdot\|$ denotes the Euclidean norm for vectors and matrices. $(.)^*$ is reserved for denoting conjugate of complex numbers and the phase of a complex number is represented by $\arg\{\cdot\}$. The μ^{th} column and the η^{th} row of matrix $\mathbf{A}$ are denoted, respectively, as $\mathbf{A}_{:,\mu}$ and $\mathbf{A}_{\eta,:}$.

For simplicity, the normalized cyclic frequency values ranging from 0 to 1 Hz. are used throughout the thesis.

1.1 History of Designing Waveforms Having Constrained Spectra

There exists a vast literature about spectrally constrained radar transmit waveform design. In this subsection, we briefly review only the most relevant works as summarized below.

In (Lindenfeld, 2004), both transmit and receive radar waveforms are designed. The transmit radar waveform is designed by constructing a penalty function which determines the amount of suppression in particular stopband frequencies. The developed algorithm is based on Fourier transform (FT). Before generating the transmit waveform, the set of suppressed frequency bands are specified. Over each frequency band, the energy level of the spectrum are decreased iteratively. In the proposed algorithm, determination of frequency stopbands is accomplished by defining a Hermitian Toeplitz matrix. In that study, a receive radar waveform is also designed along with the generated transmit waveform.

In the approach proposed in (Wang & Lu, 2011), suppressing the required frequency stopbands and reducing the correlation sidelobe levels at desired lags are traded-off by introducing a weighting factor. Through the weighting factor, suppression in time and frequency domains are performed by favoring one of them over the other on the basis of application requirements. After that, the proposed method is generalized for MIMO radar systems. This work also inspired the development of SCAN algorithm (He et al., 2010) covered in detail in the next section.

In (Wang & Lu, 2010), particle swarm optimization (PSO) algorithm is utilized to design waveforms owning orthogonal sparse frequencies for MIMO radar systems. The PSO algorithm ensures that the transmit waveforms satisfy the desired sparse frequency property and good correlation properties of having low sidelobe levels for both auto-correlation and cross-correlation functions. Designed transmit waveforms are formed by controlling the phase of sequence elements which have constant modulus.

In (Song et al., 2015), it is aimed to minimize the exact metric of integrated sidelobe level (ISL) instead of forming an approximate optimization solution similar to cyclic algorithm-new (CAN) proposed in (Stoica et al., 2009). This method strives to directly minimize the ISL metric monotonically. The algorithm derived in the end is called monotonic minimizer for integrated sidelobe level (MISL). The MISL algorithm employs the so-called majorization-minimization (MM) method which is implemented using the fast Fourier Transform (FFT). The MM method aims to provide a solution by converting a formidable minimization problem into a series of simple problems.

In (Aubry et al., 2016), an alternative technique is proposed to compose signals for increased performance in terms of signal to interference plus noise ratio (SINR). The proposed technique aims to decrease interference in particular bands which are utilized by both radar and communication signals in a shared fashion.

Designing radar transmit waveforms by defining some masks which provide a desired spectrum shape is introduced in (Patton et al., 2012). In that method, radar waveforms are designed in order to decrease the transmitted energy in the stopband with the help of a penalty function which is implemented via the discrete-time Fourier Transform (DTFT).

According to (Liang et al., 2015), to obtain the maximum amount of transmitted power in active sensing, the waveforms of interest should have constant modulus. The purpose of that study is to prevent mutual interferences of employed radio frequencies by satisfying both frequency and time domain constraints. To overcome the interference problem, the authors offer an approach which forms the designed waveforms through Lagrange programming neural network (LPNN) which separately forms the real and imaginary parts of a waveform.

In (Clancy & Walker, 2006), OFDM signals are generated in accordance with a desired signal spectrum. By modulating the transmitted power via each sub-carrier, the final ODFM signal is formed.

Except for the above mentioned studies, some additional works also exist about designing sequences having good correlation properties and desirable spectral characteristics. For instance, in (Petrolati et al., 2012), the formulation of the so-called PAT sequences is introduced. These sequences are fixed sequences with well-defined phase formulations. Performance of PAT sequences is compared against similar type of existing radar sequences such as Frank sequence and P1, P2, and Px sequences (Levanon & Mozeson, 2004).

CHAPTER TWO
SCAN AND SHAPE ALGORITHMS FOR DESIGNING RADAR TRANSMIT SEQUENCES

In this chapter, we review the algorithms of SCAN and SHAPE from the existing literature and provide numerical examples for SISO systems.

2.1 SCAN Algorithm

The SCAN algorithm was proposed for designing unimodular (i.e. constant modulus) sequences by applying constraints both in temporal and spectral domains (He et al., 2010). SCAN can be computed by utilizing FFT, and hence, is computationally quite efficient. Another advantage of the SCAN algorithm is that it can be initialized by random phased unimodular sequences of large lengths. Every realization of the algorithm with a random initialization produces a different new sequence with similar good properties.

Let us assume that the spectrum of the complex valued length-N radar transmit sequence, $x[n]$, for $n = 1,2,\ldots,N$, to be designed has stopbands (notches) in the following set of normalized frequency bands

$$\Omega = \bigcup_{s=1}^{N_s}(f_{s1}, f_{s2}) \tag{2.1}$$

where (f_{s1}, f_{s2}) corresponds to the s^{th} stopband and N_s is the number of stopbands. The number of samples, $\tilde{N}$, for calculating the discrete Fourier transform (DFT) is chosen large enough for densely covering Ω. Here, the $(n,m)^{\text{th}}$ element of $\tilde{N}\times\tilde{N}$ DFT matrix $\mathbf{F}_{\tilde{N}}$ can be given as

$$\mathbf{F}_{\tilde{N}}[n,m] = \frac{1}{\sqrt{\tilde{N}}}\mathrm{e}^{j2\pi\frac{nm}{\tilde{N}}}, \quad n,m = 0,\ldots,\tilde{N}-1. \tag{2.2}$$

A matrix $\mathbf{S}$ is created by including the columns of $\mathbf{F}_{\tilde{N}}$ corresponding to only the normalized frequencies within Ω. Another matrix $\mathbf{G}$ is formed by the remaining columns of $\mathbf{F}_{\tilde{N}}$. Then, suppression of spectral power of $x[n]$ in Ω can be realized by solving the following minimization problem (He et al., 2010)

$$\begin{aligned} &\min_{\mathbf{x},\boldsymbol{\alpha}} J_1(\mathbf{x},\boldsymbol{\alpha}) = \left\|\tilde{\mathbf{x}} - \mathbf{G}\boldsymbol{\alpha}\right\|^2 \\ &\text{subject to} \quad |x[n]| = 1 \quad n = 1,\ldots,N \end{aligned} \tag{2.3}$$

where $\tilde{\mathbf{x}} = [x[1] \ \ldots \ x[N] \ \ 0 \ \ldots \ 0]^T_{\tilde{N}\times 1}$ and $\boldsymbol{\alpha}$ is a vector of auxiliary variables. In addition to spectral suppression, SCAN can also manage to reduce autocorrelation sidelobes of $x[n]$ by utilizing the CAN (cyclic algorithm-new) algorithm (Stoica et al., 2009). CAN aims to minimize the performance metric of integrated sidelobe level (ISL) which is defined (Stoica et al., 2009) as

$$\mathrm{ISL} = 2\sum_{k=1}^{N-1} |r_x[k]|^2. \tag{2.4}$$

The merit factor (MF) is defined in (Stoica et al., 2009), (He et al., 2012) as,

$$\mathrm{MF} = \frac{|r_x[0]|^2}{\sum\limits_{\substack{k=-(N-1) \\ k\neq 0}}^{N-1} |r_x[k]|^2}. \tag{2.5}$$

In Eqn. (2.4), $r_x[k]$ denotes the aperiodic autocorrelation of $x[n]$. It is defined (Stoica et al., 2009) as

$$r_x[k] = \sum_{n=k+1}^{N} x[n]x^*[n-k] = r_x^*[-k] \ , \ \ k = 0,\ldots,N-1. \tag{2.6}$$

Utilizing $2N \times 2N$ DFT matrix $\mathbf{F}_{2N}$, suppression of autocorrelation sidelobes can be accomplished by solving the following minimization problem (He et al., 2010)

$$\begin{aligned} &\min_{\mathbf{x},\mathbf{v}} J_2(\mathbf{x},\mathbf{v}) = \left\|\mathbf{F}_{2N}^H \begin{bmatrix} \mathbf{x} \\ \mathbf{0}_{N\times 1} \end{bmatrix} - \mathbf{v}\right\|^2 \\ &\text{subject to} \quad |x[n]| = 1, \quad n = 1,\ldots,N \\ &\qquad\qquad |v[n]| = \frac{1}{\sqrt{2}}, \quad n = 1,\ldots 2N \end{aligned} \tag{2.7}$$

where $\mathbf{x} = [x[1] \ x[2] \ \ldots \ x[N]]^T$ is the designed sequence and $\mathbf{v} = [v[1] \ v[2] \ \ldots \ v[2N]]^T$ is a constant-valued vector.

The two minimization problems in Eqns. (2.3) and (2.7) can be brought together so that both spectral stopband and temporal autocorrelation sidelobe constraints are combined in a single minimization problem which can be formulated (He et al., 2010) as

$$\begin{aligned} \min_{\mathbf{x},\boldsymbol{\alpha},\mathbf{v}} J(\mathbf{x},\boldsymbol{\alpha},\mathbf{v}) &= \lambda \left\| \tilde{\mathbf{x}} - \mathbf{G}\boldsymbol{\alpha} \right\|^2 + (1-\lambda) \left\| \mathbf{F}_{2N}^H \begin{bmatrix} \mathbf{x} \\ \mathbf{0}_{N\times 1} \end{bmatrix} - \mathbf{v} \right\|^2 \\ \text{subject to} \quad |x[n]| &= 1, \quad n = 1,\ldots,N \\ |v[n]| &= \frac{1}{\sqrt{2}}, \quad n = 1,\ldots,2N \end{aligned} \tag{2.8}$$

where $0 \leq \lambda \leq 1$ is a weighting factor controlling the relative weight of the two cost functions J_1 and J_2.

2.1.1 Simulation Examples for SCAN Algorithm

In this section, we perform SCAN algorithm to suppress a predetermined spectral band. We design a unimodular sequence of length $N = 100$ along with a spectral notch. The spectral notch is placed in the range of normalized frequencies $\Omega = [0.35, 0.45)$. The weighting factor λ representing the trade-off between temporal and spectral constraints is chosen as $\lambda = 0.8$ preferring spectral suppression more. The SCAN algorithm is initialized by a realization of uniformly distributed random phased unimodular sequence with length $N = 100$. In the implementation phase, the DFT size of the SCAN algorithm is assigned as 1000 to densely cover all the frequency band. The number of iterations is fixed beforehand as 10^5 in all the simulation examples below.

For the first design example, the spectra of initial and final designed sequences are shown in Figure 2.1. To observe temporal suppression of autocorrelation sidelobes, initial and designed autocorrelations are shown in Figure 2.2.

After observing autocorrelations and spectra of sequences, we can state that both autocorrelation and spectrum of the designed sequence are suppressed compared to autocorrelation and spectrum of initial sequence, respectively.

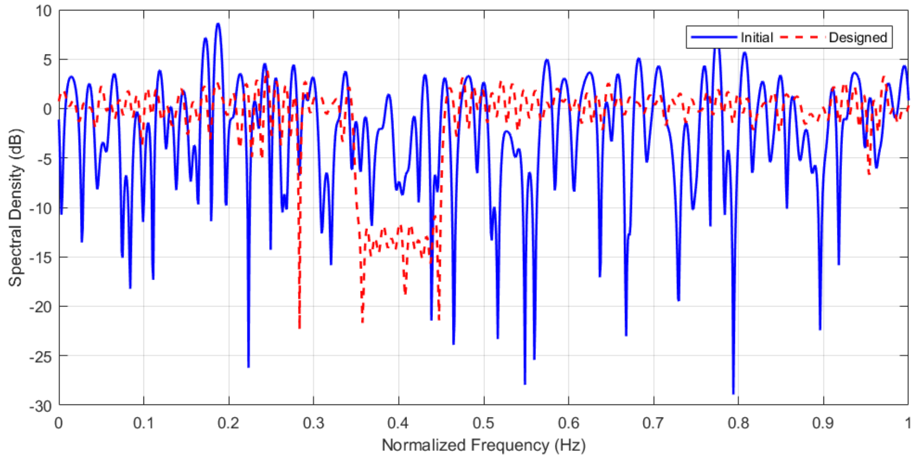

Figure 2.1 Initial and final designed spectra via SCAN algorithm with length $N = 100$ and weighting factor $\lambda = 0.8$. The spectrol notch is at $\Omega = [0.35, 0.45)$ Hz

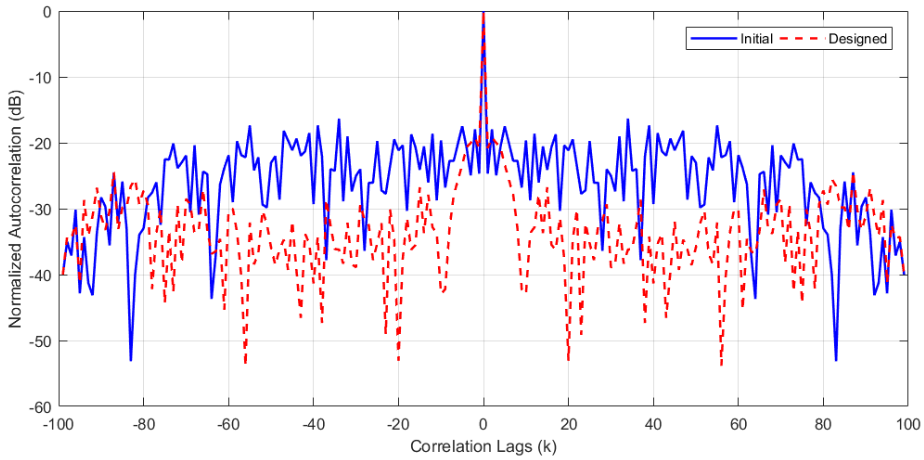

Figure 2.2 Autocorrelations of initial and final designed sequences via SCAN algorithm with length $N = 100$ and weighting factor $\lambda = 0.8$

If the weighting factor λ is allowed to have a slightly larger value for each different realization, spectral suppression becomes better in contrast to suppression of temporal autocorrelation sidelobes. To observe this trade-off effect, we employ different weighting factor, λ, values between 0.1 and 1 in the same simulation example above. The resultant ISL values are plotted in Figure 2.3.

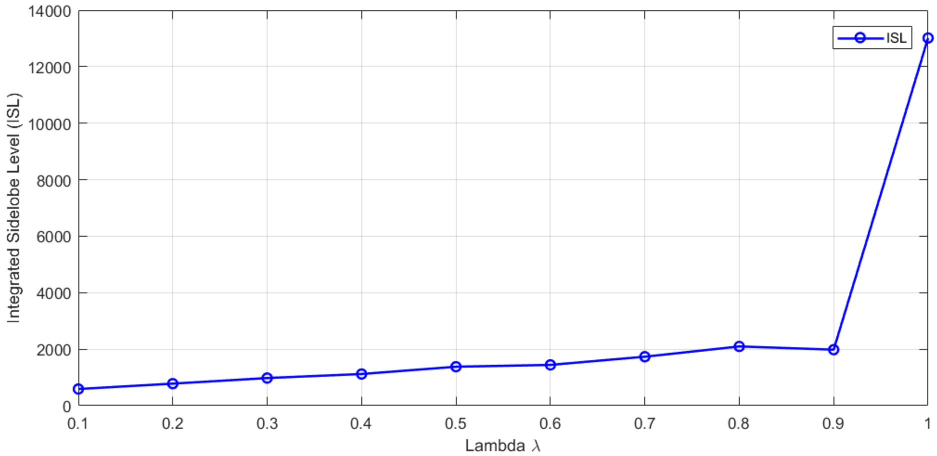

Figure 2.3 The obtained ISL values with respect to changing weighting factor values between $\lambda = 0.1$ and $\lambda = 1$

As the value of the weighting factor, λ, increases, the amount of temporal suppression decreases. Consequently, low temporal suppression leads to a higher ISL value. As a result of the trade-off between suppression in spectral and temporal domains, as long as the value of λ increases, the resultant ISL value also increases. When the weighting factor becomes unity, $\lambda = 1$, no temporal suppression occurs and the ISL value suddenly jumps to a very high value.

In our second simulation example for SCAN algorithm, we design a unimodular sequence of length $N = 1000$ having multiple spectral notches in the following normalized frequency bands,

$$\Omega = [0, 0.11) \cup [0.13, 0.19) \cup [0.25, 0.36) \cup [0.40, 0.65) \cup [0.80, 0.87) \cup [0.94, 1).$$

The weighting factor is chosen as $\lambda = 0.9$ in order to favor spectral suppression more. The SCAN algorithm is initialized by a uniformly distributed random phased unimodular sequence with length $N = 1000$. The DFT size is chosen as 1000. The spectra of initial and final designed sequences are shown in Figures 2.4 and 2.5, respectively, and the autocorrelations of initial and final designed sequences are shown in Figure 2.6.

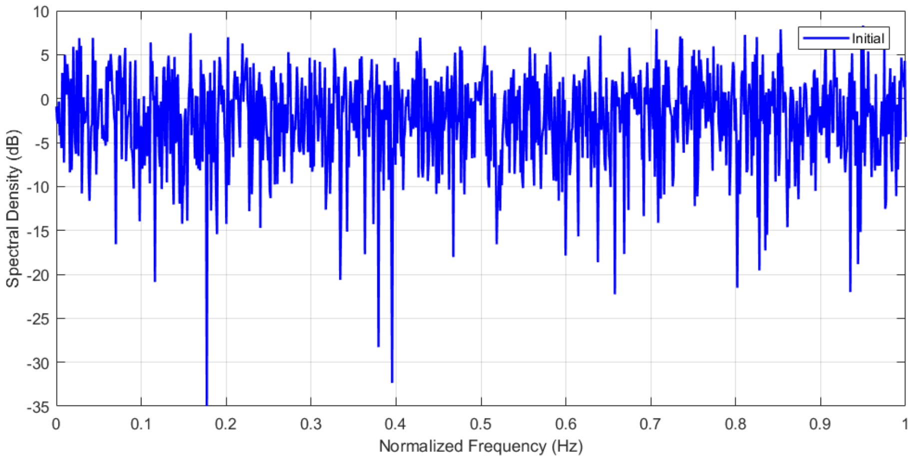

Figure 2.4 The spectrum of initial random phased sequence

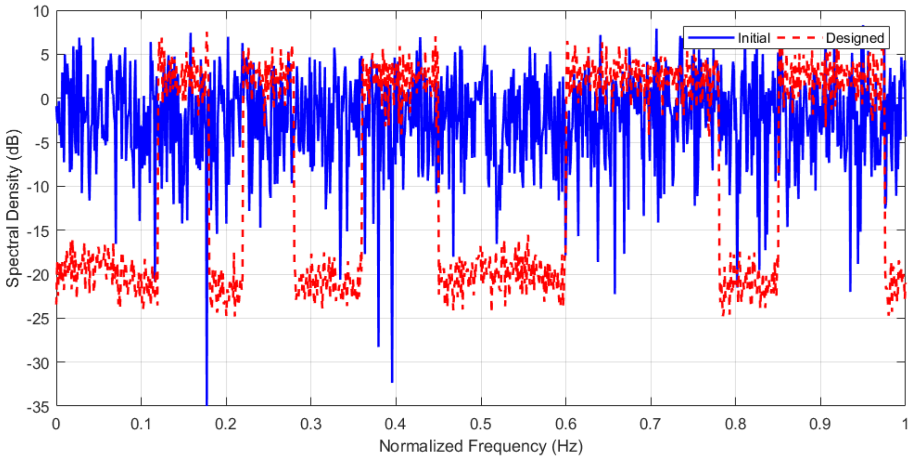

Figure 2.5 The spectrum of final designed sequence having multiple notches in $\Omega = [0, 0.11) \cup [0.13, 0.19) \cup [0.25, 0.36) \cup [0.40, 0.65) \cup [0.80, 0.87) \cup [0.94, 1)$ with $\lambda = 0.9$ and $N = 1000$

It can be seen that the designed final spectrum includes the desired suppressed notches. Note that since the value of λ is quite high, temporal suppression is of minimal amount.

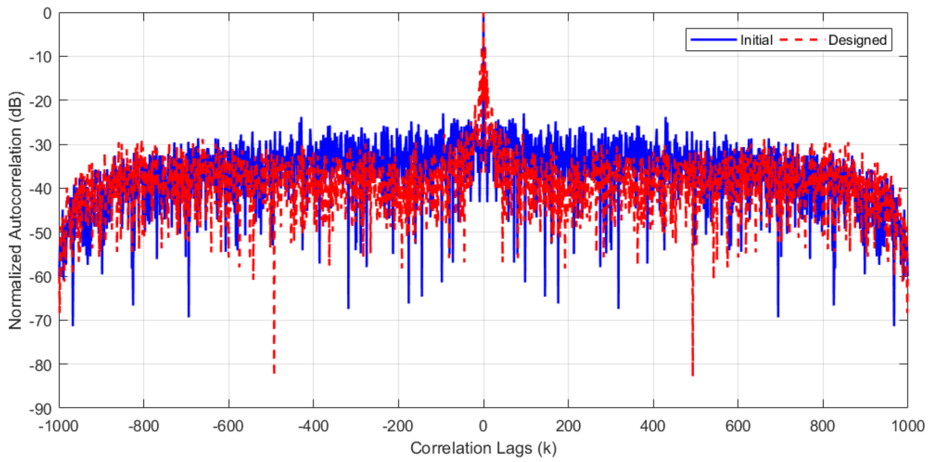

Figure 2.6 Autocorrelations of the initial and final designed sequences with $\lambda = 0.9$ and $N = 1000$

2.2 SHAPE Algorithm

Especially for wideband radar applications, designing sequences by shaping their spectrum becomes important. Unlike the SCAN algorithm, the SHAPE algorithm is purely based on spectral constraints (Rowe et al., 2014). For a wideband radar, a waveform might be required to contain notches in certain predefined spectral bands. The SHAPE algorithm can manage shaping of the spectrum in a computationally efficient manner by employing FFT and with the aid of predefined upper and lower spectral bounds.

The cost function to be minimized can be expressed as

$$\begin{aligned} &\min_{\mathbf{x},\boldsymbol{\theta}} \quad \left\| \mathbf{F}_N^H \mathbf{x} - \mathbf{y} \odot e^{j\boldsymbol{\theta}} \right\|^2 \\ &\text{subject to } |x[n]|^2 = h[n], \text{ for } \ n = 1, \ldots, N \end{aligned} \tag{2.9}$$

where $\odot$ represents element-wise product operation, $\mathbf{x} \in \mathbb{C}^{N\times 1}$ is the designed sequence, $\mathbf{y} \in \mathbb{R}^{N\times 1}$ is the nonnegative valued desired spectrum magnitude, and $\mathbf{F}_N \in \mathbb{C}^{N\times N}$ represents the unitary DFT matrix. $\boldsymbol{\theta} \in \mathbb{R}^{N\times 1}$ is an auxiliary phase vector. The constant modulus constraint is signified by $\mathbf{h} = [h[1]\ h[2]\ \ldots\ h[N]\,]^T$ which could be formed by utilizing common window functions (rectangular, raised cosine, triangular, etc.) (Rowe et al., 2014).

Instead of fitting to an exact spectrum as $\mathbf{y}$ in Eqn. (2.9), one can allow the amplitude of the spectrum to stay between an upper spectral bound, $u(f)$, and a lower spectral bound, $l(f)$. These bound functions can be approximated as vectors $\mathbf{u} = [u[1]\ u[2]\ \ldots\ u[N]\,]^T$ and $\mathbf{l} = [l[1]\ l[2]\ \ldots\ l[N]\,]^T$ sampled on the used frequency grid points. Relaxing on the exact spectrum shape by employing bounds makes the problem easier and more manageable. Thus, one can search for a spectrum, $\mathbf{z}$, with its modulus contained within the upper and lower spectral bounds. The accordingly modified minimization problem becomes (Rowe et al., 2014)

$$
\begin{aligned}
\min_{\mathbf{x},\beta,\mathbf{z}} \quad & \left\|\mathbf{F}_N^H\mathbf{x} - \beta\mathbf{z}\right\|^2 \\
\text{subject to } |x[n]|^2 &= h[n], \text{ for } n = 1,\ldots,N \\
|z[n]| &\leq u[n], \text{ for } n = 1,\ldots,N \\
|z[n]| &\geq l[n], \text{ for } n = 1,\ldots,N.
\end{aligned}
\tag{2.10}
$$

In Eqn. (2.10), β is an auxiliary scale factor which is introduced to compensate for any likely energy mismatch and phase offset between the designed time domain sequence, $\mathbf{x}$, and the spectrum, $\mathbf{z}$.

2.2.1 Simulation Examples for SHAPE Algorithm

In this section, we employ the SHAPE algorithm to design sequences with suppressed spectral bands. In our first example, we design a unimodular sequence of length $N = 100$ having only one spectral notch. We would like to note again that the SHAPE algorithm merely deals with spectral suppression ignoring any temporal suppression. The SHAPE algorithm is initialized by a realization of uniformly distributed random phased unimodular sequence with length $N = 100$. The spectral notch is placed in the normalized frequency interval of $\Omega = [0.35, 0.45)$. We employ spectral upper bound of -10 dB over the passband and -30 dB in the stopband. In this simulation example, no spectral lower bound is employed. In order to terminate the algorithm, the total number of iterations is fixed as 10^5. The envelope constraint is chosen as a regular rectangular window, $\mathbf{h} = [1\ 1\ \ldots\ 1\,]^T$. The spectra of initial and designed final sequences are shown in Figure 2.7. The employed spectral upper bound is shown using a green line. It can be seen that the SHAPE algorithm puts a notch at the required frequency band and forces the whole spectrum below the upper spectral bound.

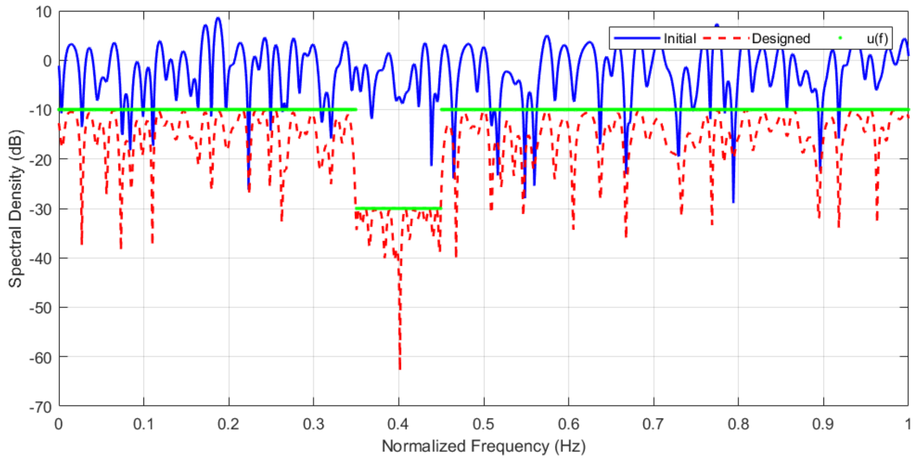

Figure 2.7 The spectra of initial and desined final sequences when the frequency stopband located in $\Omega = [0.35, 0.45)$ and with $N = 100$

In our second example, we design a unimodular sequence of length $N = 1000$ having multiple spectral notches. We choose the six normalized frequency stopbands as

$$\Omega = [0, 0.11) \cup [0.13, 0.19) \cup [0.25, 0.36) \cup [0.40, 0.65) \cup [0.80, 0.87) \cup [0.94, 1).$$

The SHAPE algorithm is initialized by a uniformly distributed random phased unimodular sequence with length $N = 1000$. We utilize spectral upper bounds of -10 dB in the passband and of -30 dB in the stopband, respectively. No lower spectral bound is utilized. As the envelope constraint, we choose a regular rectangular window, $\mathbf{h} = [1\ 1\ \dots\ 1\,]^T$. To stop the algorithm, the total number of iterations is determined in advance as 10^5. The spectra of initial and final designed sequences are shown in Figure 2.8. The employed spectral upper bound is shown using a green line. Again, the algorithm is able to form the desired notches and keep the designed spectrum below the employed upper spectral bound.

2.3 Comparison of SCAN and SHAPE Algorithms

We perform a simulation example to compare performances of SCAN and SHAPE algorithms. In this example, we assign the value of the parameter λ in the SCAN

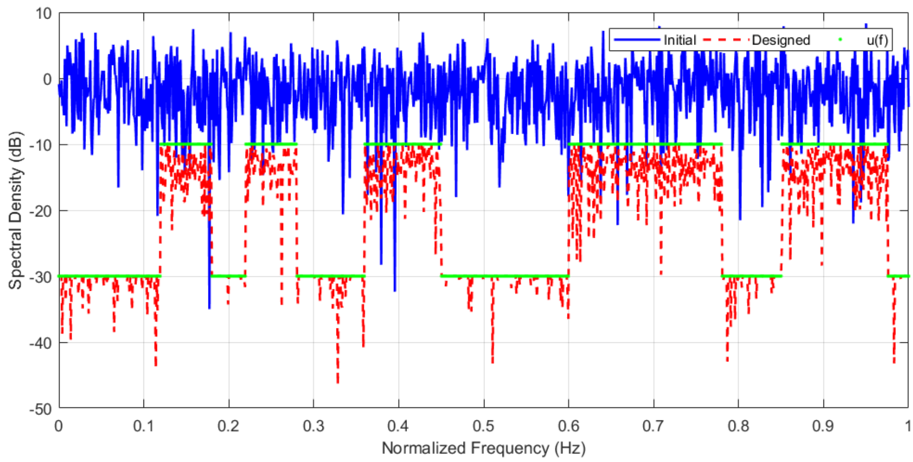

Figure 2.8 The spectra of initial and final designed sequences with $N = 1000$

algorithm as unity ($\lambda = 1$). Thus, the temporal correlation constraint is completely removed and the SCAN algorithm performs the sequence design based solely on the spectral constraint. Using both SCAN and SHAPE algorithms, we design unimodular sequences of length $N = 100$ with a spectral notch in the normalized frequency band of $\Omega = [0.5, 0.55)$. Both algorithms are initialized with the same realization of a uniformly distributed random phased unimodular sequence with length $N = 100$. In implementing both algorithms, we perform DFTs of length 1000. In the SHAPE algorithm, we employ a spectral upper bound of -10 dB over the passband and of -30 dB in the stopband. We employ no lower spectral bound. The envelope constraint is chosen as a regular rectangular window $\mathbf{h} = [1 \ 1 \ \ldots \ 1\,]^T$. To compare both algorithms on an equal footing, the number of iterations is fixed beforehand as 10^5. The spectra of initial and final designed sequences are shown in Figures 2.9 and 2.10. Figure 2.9 shows the spectra of the initial and the final designed sequences by the SCAN algorithm. Similarly, Figure 2.10 displays the spectra of the initial and final designed sequences by the SHAPE algorithm. The employed spectral upper bound is shown using a green line.

By looking at the spectra of the final designed sequences, we can say that SCAN produces a deeper notch (approximately -60 dB) than the SHAPE algorithm in which the depth of the notch is determined by the given spectral upper bound. In contrast, the SCAN algorithm does not require employment of any spectral bounds.

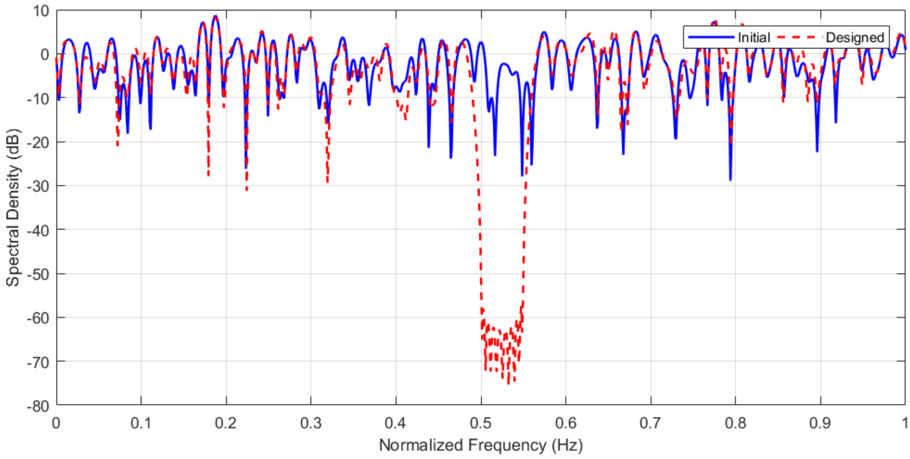

Figure 2.9 The spectra of initial and final designed sequences via SCAN algorithm with N = 100 and $\lambda = 1$

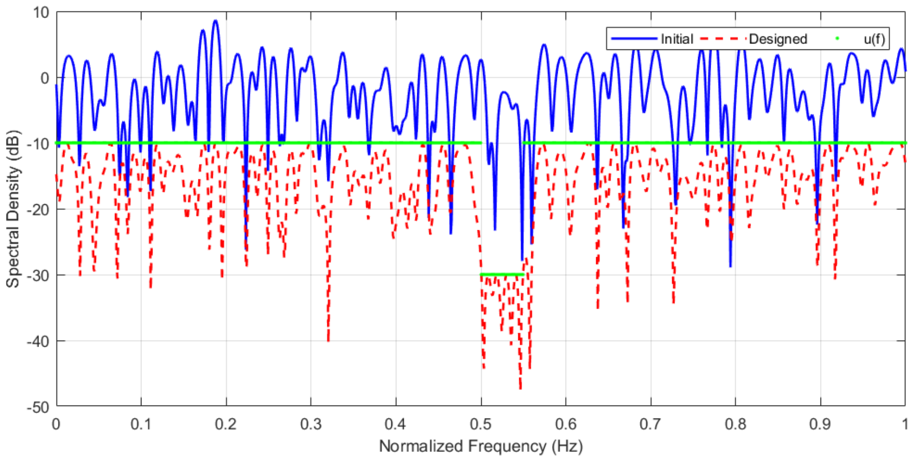

Figure 2.10 The spectra of initial and final designed sequences via SHAPE algorithm with N = 100

CHAPTER THREE
EXTENSIONS TO MIMO

In this chapter, we extend the formulations of SCAN and SHAPE algorithms for MIMO systems. In generalizing SISO versions of SCAN and SHAPE algorithms, we have been inspired by (He et al., 2009) and (He et al., 2012) where the CAN algorithm was generalized into MIMO systems. Thanks to using mutually orthogonal transmit sequences, MIMO radar systems might provide better detection performance, improved parameter estimation, and better resolution (He et al., 2012).

Both MIMO SCAN and MIMO SHAPE algorithms are initialized with a set of sequences which can be represented as columns of a matrix as follows

$$\mathbf{X}^{(0)} = [\,\mathbf{x}_1\,|\,\mathbf{x}_2\,|\,\ldots\,|\mathbf{x}_M]_{N\times M} \tag{3.1}$$

where the m^{th} column represents the m^{th} initial sequence $\mathbf{x}_m = [x_m[1]\ x_m[2]\ \ldots\ x_m[N]\,]^T$. Note that there are M initial sequences of length N.

Aperiodic cross-correlation of two sequences $\mathbf{x}_{m_1}$ and $\mathbf{x}_{m_2}$ can be defined (He et al., 2012) as

$$r_{m_1 m_2}[k] = \sum_{n=k+1}^{N} x_{m_1}[n]x^*_{m_2}[n-k] = r^*_{m_1 m_2}[-k] \tag{3.2}$$

where $m_1, m_2 = 1,2,\ldots,M$ and $n = 1,2,\ldots,N$. It is desired to have low level cross-correlations between designed transmitted sequences.

The cross-energy spectral density (CESD), $P_{m_1,m_2}(f)$, on the other hand, can be defined (Alessio, 2015) via the DTFT of $r_{m_1,m_2}[k]$ as

$$P_{m_1,m_2}(f) = \sum_{k=-\infty}^{\infty} r_{m_1,m_2}[k]e^{-j2\pi fk}. \tag{3.3}$$

3.1 MIMO SCAN Algorithm

In this section, we extend the SCAN algorithm in order to design transmit sequences for MIMO radar systems. In MIMO sequence design formulations, operations on vectors are generalized into matrix operations. This is because the MIMO SCAN algorithm is initialized by multiple sequences which are arranged in the form of a matrix as shown in Eqn. (3.1).

To begin, we assume that the spectrum of the complex valued $N \times M$ radar transmit matrix $\mathbf{X}$ to be designed has stopbands in the normalized frequency bands, Ω, as defined previously in Eqn. (2.1). Similarly, the $(n,m)^{\text{th}}$ element of the $\tilde{N} \times \tilde{N}$ DFT matrix, $\mathbf{F}_{\tilde{N}}$, is defined as in Eqn. (2.2) in the previous chapter.

A matrix $\mathbf{S}$ is created by including the columns of $\mathbf{F}_{\tilde{N}}$ corresponding to only the normalized frequencies within Ω. Another matrix $\mathbf{G}$ is formed by the remaining columns of $\mathbf{F}_{\tilde{N}}$. Then, suppression of spectral power of $\mathbf{X}$ in Ω can be realized by solving the following minimization problem (He et al., 2010)

$$\begin{aligned} &\min_{\mathbf{X},\boldsymbol{A}} J_1(\mathbf{X},\boldsymbol{A}) = \left\|\tilde{\mathbf{X}} - \mathbf{G}\boldsymbol{A}\right\|^2 \\ &\text{subject to} \quad |X[n,m]| = 1 \quad n = 1,\ldots,N \\ &\qquad\qquad\qquad\qquad\qquad\quad m = 1,\ldots,M \end{aligned} \tag{3.4}$$

where $\tilde{\mathbf{X}} = \begin{bmatrix} \mathbf{X}_{N\times M} \\ \mathbf{0}_{(\tilde{N}-N)\times M} \end{bmatrix}_{\tilde{N}\times M}$ and $\mathbf{A}$ is a matrix of auxiliary variables.

Similar to its SISO counterpart, the MIMO SCAN algorithm can also perform temporal suppression on autocorrelation sidelobes of the designed sequences in $\mathbf{X}_{N\times M}$ by implementing the CAN algorithm for multiple initial sequences as shown in (He et al., 2012). Utilizing the $2N \times 2N$ DFT matrix $\mathbf{F}_{2N}$, suppression of autocorrelation sidelobes can be realized successfully by solving the following optimization problem

$$\begin{aligned} &\min_{\mathbf{X},\mathbf{V}} J_2(\mathbf{X},\mathbf{V}) = \left\|\mathbf{F}_{2N}^H \begin{bmatrix} \mathbf{X} \\ \mathbf{0}_{N\times M} \end{bmatrix} - \mathbf{V}\right\|^2 \\ &\text{subject to} \quad |X[n,m]| = 1, \quad n = 1,\ldots,N \\ &\qquad\qquad\qquad\qquad\qquad\quad m = 1,\ldots,M \\ &\qquad\qquad |V[n,m]| = \frac{1}{\sqrt{2}}, \quad n = 1,\ldots 2N \\ &\qquad\qquad\qquad\qquad\qquad\quad m = 1,\ldots,M \end{aligned} \tag{3.5}$$

where $\mathbf{X} = [\, \mathbf{x}_1 \mid \mathbf{x}_2 \mid \dots \mid \mathbf{x}_M]_{N\times M}$ is the matrix of designed sequences and $\mathbf{V} = [\, \mathbf{v}_1 \mid \mathbf{v}_2 \mid \dots \mid \mathbf{v}_M]_{2N\times M}$ is a constant-valued matrix.

Both minimization problems in Eqns. (3.4) and (3.5) can be combined using a weighting factor λ creating a single minimization problem. Thus, spectral suppression at normalized frequency stopbands and temporal suppression of autocorrelation sidelobes can be accomplished in a single minimization problem as follows

$$\begin{aligned}
\min_{\mathbf{X},\boldsymbol{A},\mathbf{V}} J(\mathbf{X},\boldsymbol{A},\mathbf{V}) = \lambda \left\| \tilde{\mathbf{X}} - \mathbf{G}\boldsymbol{A} \right\|^2 + (1-\lambda) \left\| \mathbf{F}_{2N}^{H} \begin{bmatrix} \mathbf{X} \\ \mathbf{0}_{N\times 1} \end{bmatrix} - \mathbf{V} \right\|^2 & \\
\text{subject to} \quad |X[n,m]| = 1, \quad n = 1,\dots,N & \\
m = 1,\dots,M & \\
|V[n,m]| = \frac{1}{\sqrt{2}}, \quad n = 1,\dots,2N & \\
m = 1,\dots,M &
\end{aligned} \tag{3.6}$$

where $0 \leq \lambda \leq 1$ is the weighting factor controlling the relative weight of the two cost functions J_1 and J_2.

3.1.1 Steps of MIMO SCAN Algorithm

Before outlining the steps of the MIMO SCAN algorithm, the following input parameters are to be determined. The input matrix $\mathbf{X}_{N\times M}^{(0)}$ in (3.1) involving the initial set of sequences, the weighting parameter, λ, the DFT size of the algorithm, $\tilde{N}$, and the set of frequency bands, Ω, to be suppressed are assigned first. Then, the matrix $\mathbf{G}$ is formed as explained prior to Eqn. (3.4). After those required initializations, the steps of the MIMO SCAN algorithm can be executed as follows:

Step #1: Form the zero-padded matrix, $\tilde{\mathbf{X}}_{\tilde{N}\times M}$, in an analogous manner to $\tilde{\mathbf{x}}$ in (2.3). Then, calculate $\boldsymbol{A} = \mathbf{G}^H \tilde{\mathbf{X}}_{\tilde{N}\times M}$.

Step #2: Form the zero-padded matrix, $\mathbf{X}_{2N\times M}$, and compute $2N \times M$ matrix, $\mathbf{V} = \frac{1}{\sqrt{2}} e^{j\arg\left\{\mathbf{F}_{2N}^{H}\mathbf{X}_{2N\times M}\right\}}$.

Step #3: Rename the first N rows of $\mathbf{G}\boldsymbol{A}$ and $\mathbf{F}_{2N}\mathbf{V}$ as $\mathbf{C_1}$ and $\mathbf{C_2}$, respectively.

Step #4: Find the resultant matrix at iteration i as $\mathbf{X}^{(i)} = e^{j\arg\{\lambda \mathbf{C_1} + (1-\lambda)\mathbf{C_2}\}}$.

Iteration: Perform Step 1 through Step 4 for a predetermined number of iterations.

3.2 MIMO SHAPE Algorithm

Similar to the MIMO SCAN algorithm, we extend the SHAPE algorithm (Rowe et al., 2014) in order to become applicable for MIMO radar systems. For MIMO SHAPE algorithm, the minimization problem to be solved can be written as

$$\begin{aligned} &\min_{\mathbf{X},\,\boldsymbol{\theta}} \left\| \mathbf{F}_N^H \mathbf{X} - \mathbf{Y} \odot \mathbf{e}^{j\boldsymbol{\theta}} \right\|^2 \\ \text{subject to} \quad & |X[n,m]|^2 = h[n], \quad \text{for} \quad n = 1, \ldots, N \\ & \qquad\qquad\qquad\qquad\qquad\quad m = 1, \ldots, M \end{aligned} \tag{3.7}$$

where $\odot$ symbolizes element-wise product operation, $\mathbf{X} \in \mathbb{C}^{N\times M}$ is the designed matrix comprising unimodular radar sequences, $\mathbf{Y} \in \mathbb{R}^{N\times M}$ is the nonnegative valued desired spectra magnitude, and $\mathbf{F}_N \in \mathbb{C}^{N\times N}$ denotes the unitary DFT matrix. $\boldsymbol{\theta} \in \mathbb{R}^{N\times M}$ is an auxiliary phase matrix. The constant modulus constraint for the designed matrix is emphasized by $\mathbf{h} = [h[1]\ h[2]\ \ldots\ h[N]\,]^T$ which might be formed by employing common window functions (rectangular, raised cosine, triangular, etc.).

For the sake of simplifying the solution, lower, $l[n]$, and upper, $u[n]$, spectral bounds are incorporated into the problem as

$$\begin{aligned} \min_{\mathbf{X},\,\boldsymbol{\beta},\,\mathbf{Z}} \quad & \left\| \mathbf{F}_N^H \mathbf{X} - \boldsymbol{\beta} \odot \mathbf{Z} \right\|^2 \\ \text{subject to } & |X[n,m]|^2 = h[n], \text{ for } n = 1, \ldots, N \text{ and } m = 1, \ldots, M \\ & |Z[n,m]| \leq u[n], \text{ for } n = 1, \ldots, N \text{ and } m = 1, \ldots, M \\ & |Z[n,m]| \geq l[n], \text{ for } n = 1, \ldots, N \text{ and } m = 1, \ldots, M. \end{aligned} \tag{3.8}$$

In Eqn. (3.8), columns of $\mathbf{Z}_{N\times M}$ include the spectra of designed sequences. $\boldsymbol{\beta}_{N\times M}$ represents an auxiliary scale matrix. Each column of $\boldsymbol{\beta}$ is formed by the same element.

For example, the m^{th} column of $\boldsymbol{\beta}$ contains the elements of β_m as

$$\boldsymbol{\beta}_{:,m} = \begin{bmatrix} \beta_m \\ \vdots \\ \beta_m \end{bmatrix}_{N\times 1} . \tag{3.9}$$

MIMO SHAPE algorithm is started by the initial matrix $\mathbf{X}^{(0)}_{N\times M}$ which contains M initial sequences of length N as its columns. The m^{th} column of the $N \times M$ auxiliary scale matrix, $\boldsymbol{\beta}$, is initialized as,

$$\boldsymbol{\beta}^{(0)}_{:,m} = \begin{bmatrix} 1 \\ \vdots \\ 1 \end{bmatrix}. \tag{3.10}$$

3.2.1 Steps of MIMO SHAPE Algorithm

MIMO SHAPE algorithm is started by assigning some initial input parameters. The matrix $\mathbf{X}^{(0)}_{N\times M}$ contains M initial sequences of length N as its columns. The m^{th} column of the $N \times M$ auxiliary scale matrix, $\boldsymbol{\beta}$, is initialized as $\boldsymbol{\beta}^{(0)}_{:,m} = [1\ 1 \ldots\ 1]^T$. The upper, $\mathbf{u} = [u[1]\ u[2]\ \ldots\ u[N]\,]^T$, and lower, $\mathbf{l} = [l[1]\ l[2]\ \ldots\ l[N]\,]^T$, bound vectors for spectral suppression and the window vector, $\mathbf{h} = [h[1]\ h[2]\ \ldots\ h[N]\,]^T$, for forming time-domain envelope are assigned. After assigning these initial parameters, the steps of the MIMO SHAPE algorithm are performed as follows.

Step #1: Initialize the temporary matrix $\mathbf{Q}_{N\times M} = \mathbf{F}^H_N \mathbf{X}^{(0)}_{N\times M}$ and divide the m^{th} column of $\mathbf{Q}_{N\times M}$ by the scalar value, β_m, which is the scalar forming the m^{th} column of the $N \times M$ auxiliary scale matrix, $\boldsymbol{\beta}$.

Step #2: In parallel to the pseudocode of the SISO SHAPE algorithm given in (Rowe et al., 2014), perform comparisons of the elements in each and every column of the temporary matrix $\mathbf{Q}_{N\times M}$ with the corresponding elements of the upper, $\mathbf{u}$, and lower, $\mathbf{l}$, spectral bound vectors. Via execution of these comparisons, determine the elements of the auxiliary matrix $\mathbf{Z}^{(i)}$ at the i^{th} iteration. In these comparisons; if $\mathbf{Q}[n,m] > u[n]$, then assign $\mathbf{Z}^{(i)}[n,m] = u[n]\frac{\mathbf{Q}[n,m]}{|\mathbf{Q}[n,m]|}$; if $\mathbf{Q}[n,m] < l[n]$, then assign

$\mathbf{Z}^{(i)}[n,m] = l[n]\frac{\mathbf{Q}[n,m]}{|\mathbf{Q}[n,m]|}$. Otherwise, assign $\mathbf{Z}^{(i)}[n,m] = \mathbf{Q}[n,m]$.

Step #3: Calculate $\beta_m^{(i)}$ which is scalar forming the m^{th} column of the $N \times M$ auxiliary scale matrix, $\boldsymbol{\beta}^{(i)}$ at the i^{th} iteration using the m^{th} columns of both $\mathbf{X}^{(i-1)}$ and $\mathbf{Z}^{(i)}$, as $\beta_m^{(i)} = \frac{\mathbf{Z}^H[n,m]\mathbf{F}_N^H\mathbf{X}_{N\times M}[n,m]}{||\mathbf{Z}[n,m]||^2}$.

Step #4: Compute the m^{th} column of the matrix $\mathbf{V}^{(i)}$ by multiplying the m^{th} column of $\mathbf{F}_N\mathbf{Z}^{(i)}$ by the scalar $\beta_m^{(i)}$.

Step #5: In parallel to the pseudocode of the SISO SHAPE algorithm given in (Rowe et al., 2014), calculate the elements of the m^{th} column of $\mathbf{X}^{(i)}$ using preassigned window vector $\mathbf{h}$ and the corresponding m^{th} column of $\mathbf{V}^{(i)}$. If $\mathbf{V}[n,m] \neq h[n]$, then assign $\mathbf{X}^{(i)}[n,m] = \sqrt{h[n]}\frac{\mathbf{V}[n,m]}{|\mathbf{V}[n,m]|}$. Otherwise, assign $\mathbf{X}^{(i)}[n,m] = \mathbf{V}[n,m]$.

Step #6: Calculate $\mathbf{Q}_{N\times M} = \mathbf{F}_N^H\mathbf{X}_{N\times M}^{(i)}$ and divide the m^{th} column of $\mathbf{F}_N^H\mathbf{X}_{N\times M}^{(i)}$ by the scalar $\beta_m^{(i)}$.

Iteration: Perform Step 2 through Step 6 for a predetermined number of iterations.

CHAPTER FOUR
SIMULATION RESULTS FOR MIMO SCAN AND MIMO SHAPE ALGORITHMS

In this chapter, we present simulation examples of the MIMO SCAN and MIMO SHAPE algorithms introduced in the previous chapter. Through the examples, we compare performances of the two algorithms against each other. In all of the examples, both algorithms are initialized with uniformly distributed random phased unimodular sequences of length $N = 100$.

4.1 Simulation Examples for MIMO SCAN

The length of the sequences to be designed and the number of designed sequences are taken as $N = 100$ and $M = 2$, respectively. Thus, when finished, the algorithm produces two unimodular sequences as columns of a 100×2 matrix. The weighting factor λ introduced in Eqn. (3.6) determines the preference between the temporal and spectral constraints and is chosen as $\lambda = 0.8$ favouring spectral shaping more than lowering correlation sidelobes. A spectral notch in the normalized frequency band, $\Omega = [0.65, 0.8)$, is placed for both designed sequences. The FFT size is taken as $\tilde{N} = 1000$ and the number of iterations is fixed as 2×10^5. The spectra of the resultant first and second sequences can be seen in Figures 4.1 and 4.2, respectively. The CESD of the initial and designed sequences are plotted in Figure 4.3. It is interesting to observe that similar to the individual spectra in Figures 4.1 and 4.2, the CESD of the designed sequences in Figure 4.3 also contains a spectral notch in the required stopband. Moreover, cross-correlation of the designed sequences displayed in Figure 4.4 remains low obeying almost zero cross-correlation requirement for nearly orthogonal sequences. Finally, sidelobes of the autocorrelations of both designed sequences are greatly suppressed as indicated in Figures 4.5 and 4.6.

We can measure performance of our proposed algorithms by calculating certain performance metrics of the initial and final designed sequences. Two of those metrics

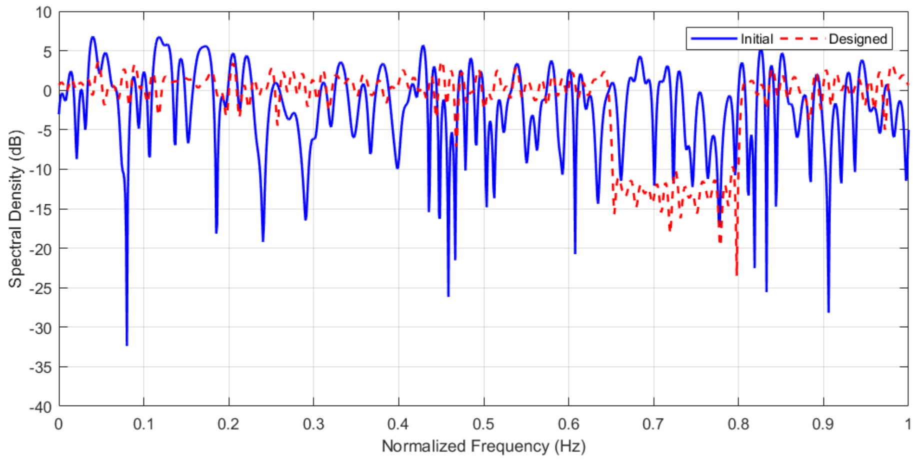

Figure 4.1 Initial and final spectra of the first designed sequence

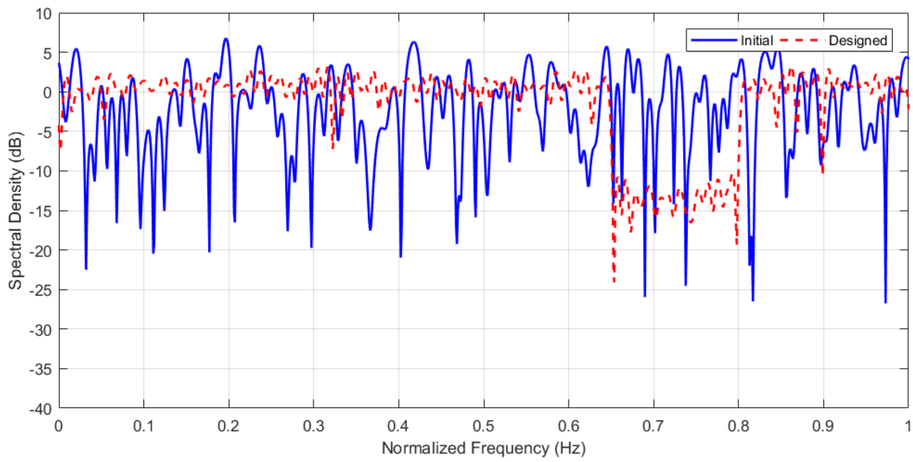

Figure 4.2 Initial and final spectra of the second designed sequence

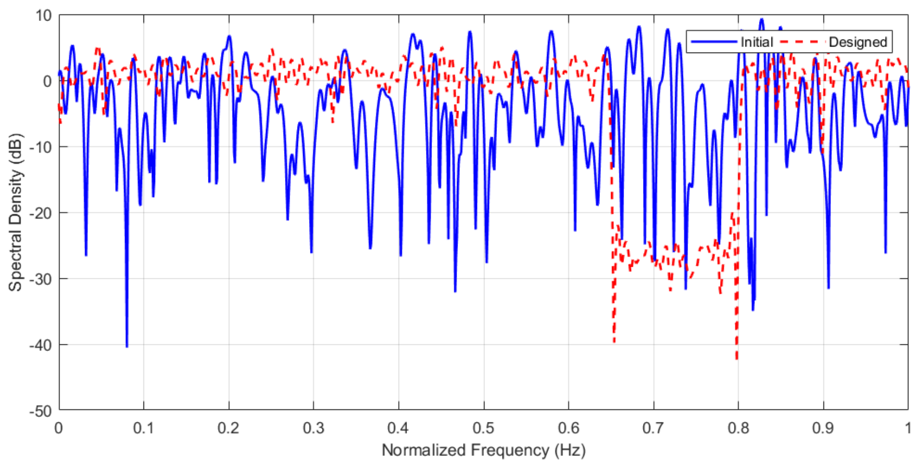

Figure 4.3 CESDs of initial and final designed sequences

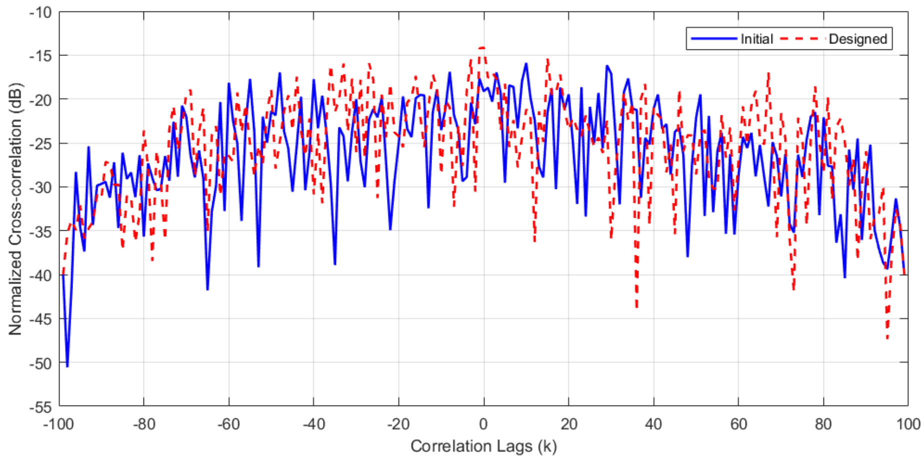

Figure 4.4 Cross-correlations of initial and final designed sequences

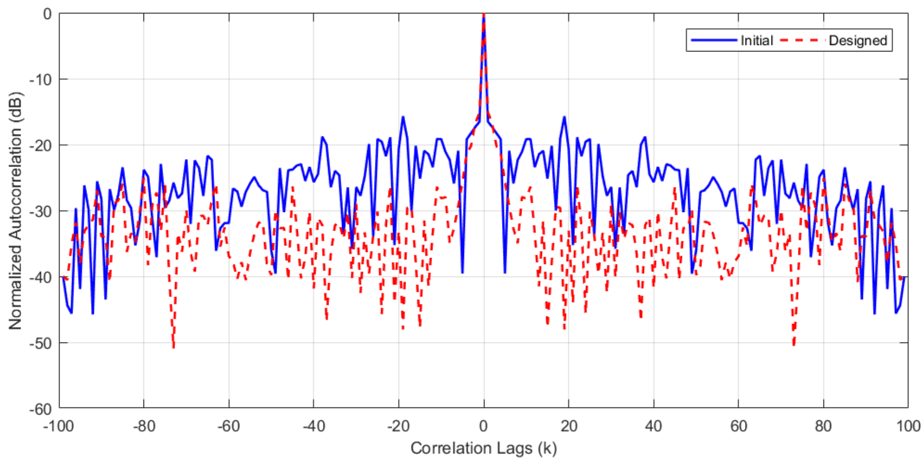

Figure 4.5 Initial and final autocorrelations of the first designed sequence

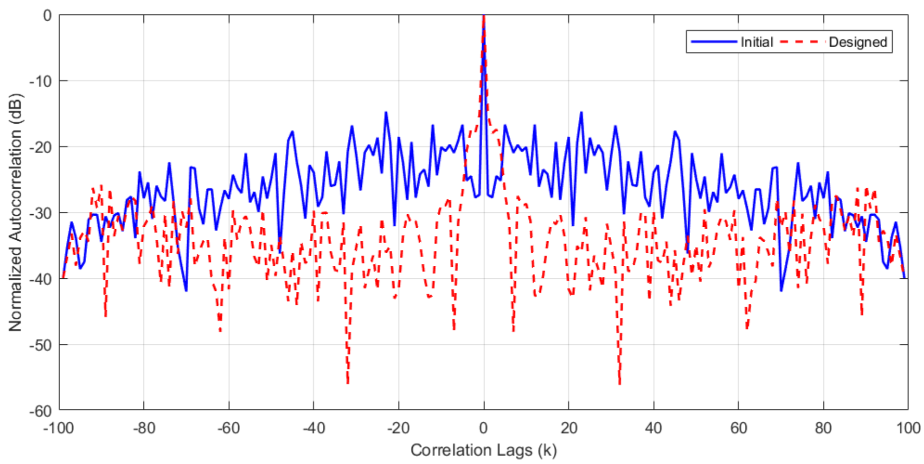

Figure 4.6 Initial and final autocorrelations of the second designed sequence

are ISL in Eqn. (2.4) and MF in Eqn. (2.5). We can also look at the stopband levels of the designed spectra to determine how effectively the design algorithm suppresses the desired frequency bands.

Table 4.1 displays the performance metrics of the initial and final sequences designed by MIMO SCAN algorithm for the weighting parameter values of $\lambda = 0.8$ and $\lambda = 0.2$. One should keep in mind that it is desirable to obtain ISL values as low as possible. Looking at Eqn. (2.8) one can see that when $\lambda < 0.5$ the MIMO SCAN algorithm constrains the correlations of the designed sequences more than their spectra. This is apparent in the last two rows of Table 4.1 for which $\lambda = 0.2$ and the ISL values are lower than that of final designed sequences for $\lambda = 0.8$. On the contrary, when $\lambda = 0.8$, spectra of the designed sequences are constrained more as indicated by the much lower stopband levels.

Similar to ISL, the metric of MF also measures suppression of autocorrelation sidelobes, although, contrary to ISL, MF is desired to be as high as possible. The third column of Table 4.1 represents MF values of the initial and final designed sequences via the MIMO SCAN algorithm. Again, the MF values of MIMO SCAN with $\lambda = 0.2$ are better compared to the values obtained when $\lambda = 0.8$.

By virtue of their definitions, the ISL and MF performance metrics are concerned with temporal autocorrelation sidelobes, but not spectral properties. Hence, to evaluate spectral performances of our proposed algorithms, we measure the stopband level in (dB) by averaging (dB) values over the corresponding stopband frequencies. Stopband level indicates the amount of spectral suppression by the design algorithm. It can be seen from the fourth column of Table 4.1 that, in contrast to ISL and MF, when the value of λ is larger, spectral suppression performance of MIMO SCAN is much better. This is because when $\lambda > 0.5$ the spectrum is constrained more than autocorrelation.

In our second example, we design three unimodular sequences by MIMO SCAN algorithm. The sample length and the number of designed sequences are taken as $N = 100$ and $M = 3$, respectively. When the algorithm terminates after a pre-determined number of iterations, the matrix $\mathbf{X}$ to be designed, is generated. The weighting factor

Table 4.1 Performance metrics of MIMO SCAN when designing two radar sequences

MIMO SCAN	ISL	MF	Stopband Level (dB)
Initial 1^{st} Sequence	8.538e+03	1.1712	-3.1252
Initial 2^{nd} Sequence	8.834e+03	1.1319	-2.2628
Final 1^{st} Sequence ($\lambda = 0.8$)	2.6824e+03	3.7280	-23.5015
Final 2^{nd} Sequence ($\lambda = 0.8$)	2.5194e+03	3.6992	-24.0894
Final 1^{st} Sequence ($\lambda = 0.2$)	1.0186e+03	9.8172	-1.9971
Final 2^{nd} Sequence ($\lambda = 0.2$)	759.7848	13.1616	-1.8820

of the MIMO SCAN algorithm is chosen as $\lambda = 0.8$. A spectral notch is placed in the normalized frequency band of $\Omega = [0.75, 0.85)$. Figures 4.7, 4.8, and 4.9 display the spectra of the initial and final designed sequences. Over the stopband frequency, the suppression is approximately -15 dB.

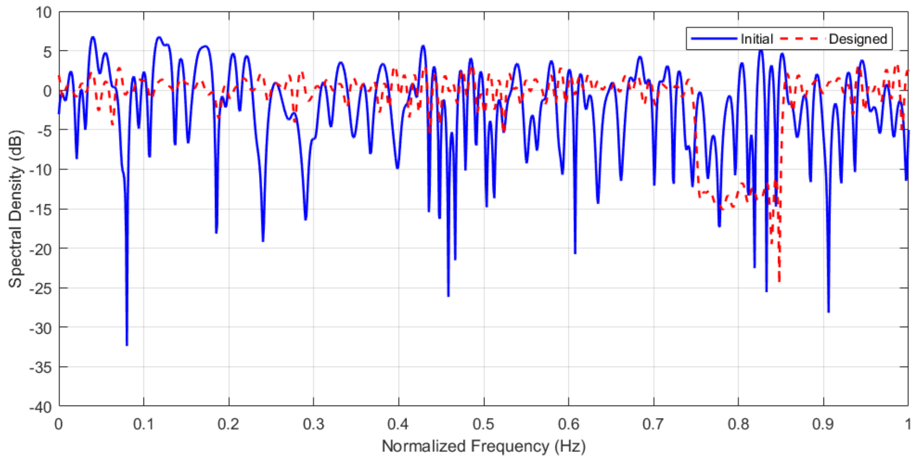

Figure 4.7 Initial and final spectra of the first designed sequence

CESDs of initial and final sequences are shown in Figures 4.10, 4.11, and 4.12 for the first and second designed sequences, the first and third designed sequences, and the second and third designed sequences, respectively. It can be seen that CESDs of the designed sequences also contain a notch at the desired stopband with an approximate power of -25 dB.

Figures 4.13, 4.14, and 4.15 exhibit cross-correlations of the inital and final

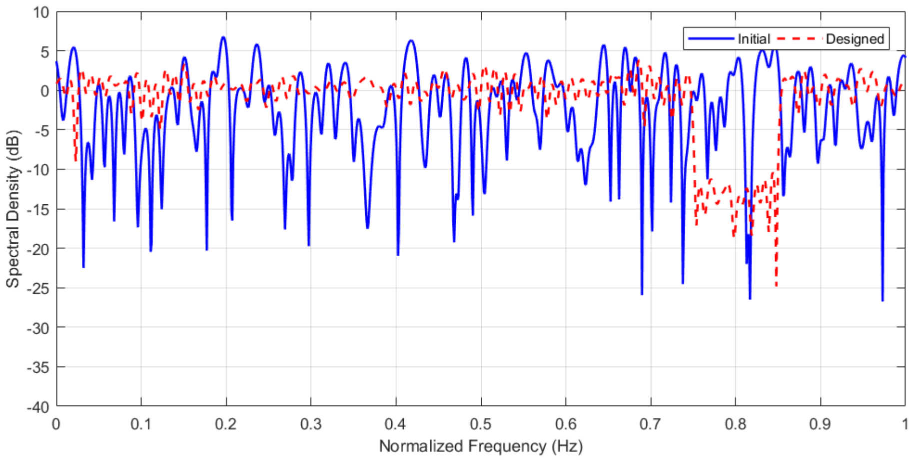

Figure 4.8 Initial and final spectra of the second designed sequence

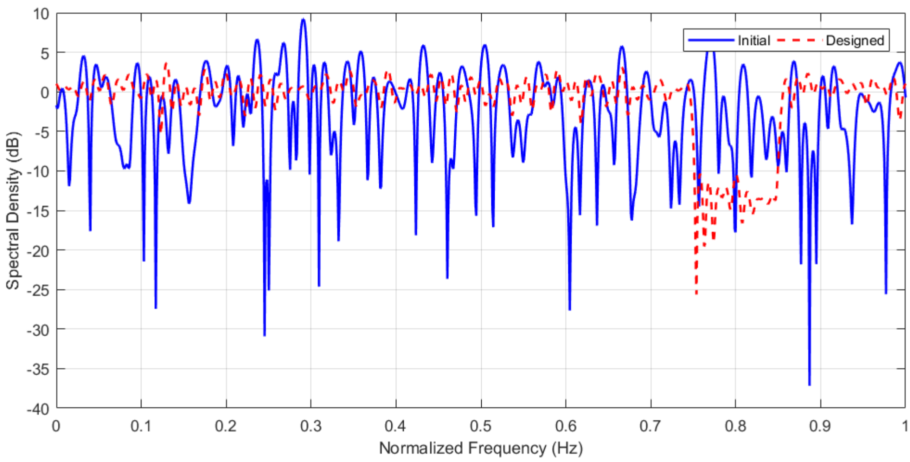

Figure 4.9 Initial and final spectra of the third designed sequence

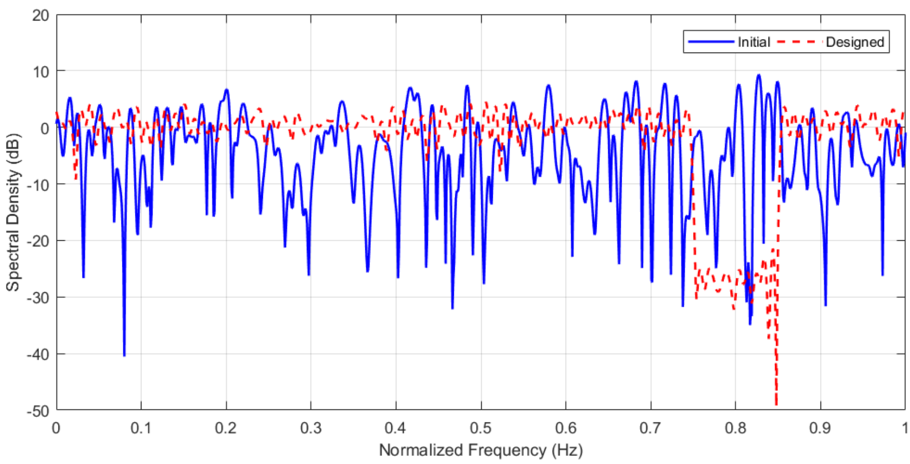

Figure 4.10 The initial and final CESDs of first and second designed sequences

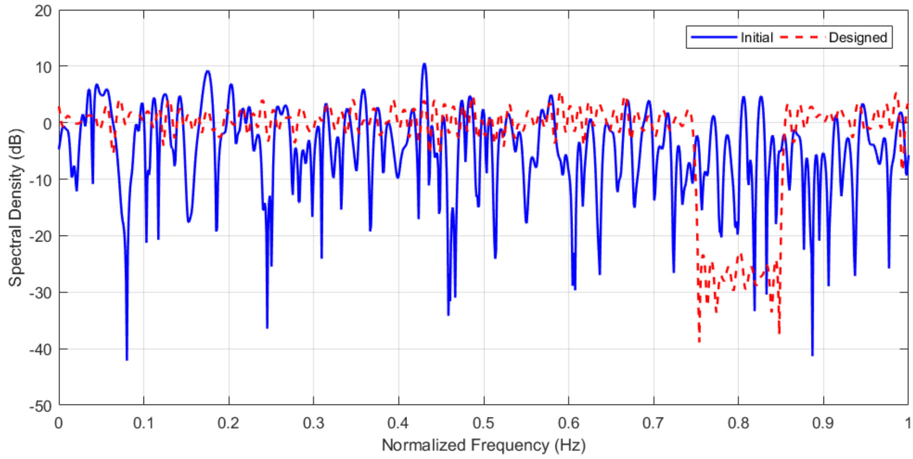

Figure 4.11 The initial and final CESDs of first and third designed sequences

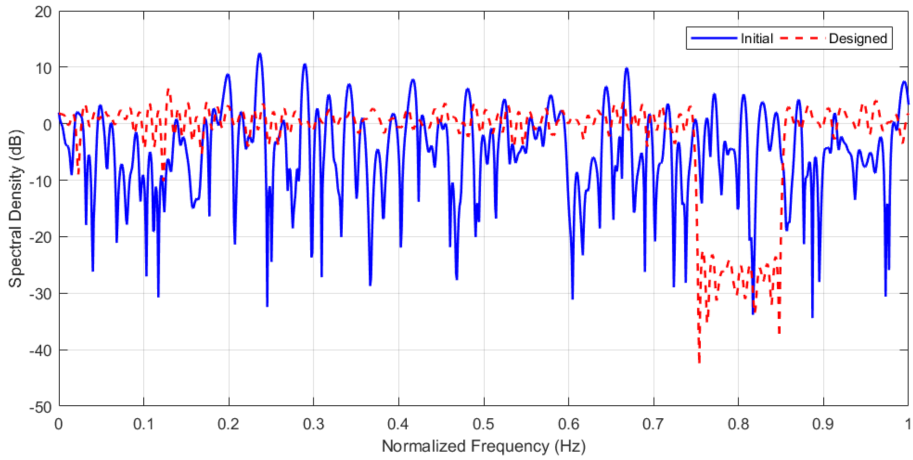

Figure 4.12 The initial and final CESDs of second and third designed sequences

sequences for the first and second designed sequences, the first and third designed sequences, and the second and third designed sequences, respectively.

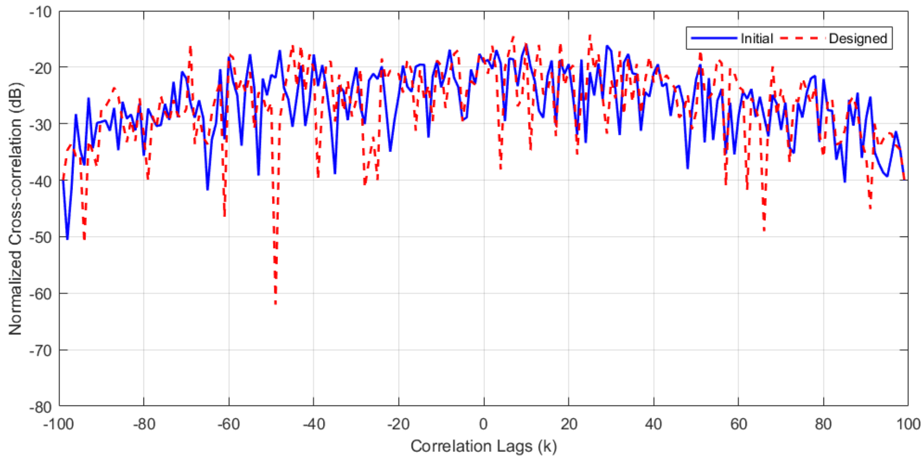

Figure 4.13 Initial and final cross-correlations of first and second designed sequences

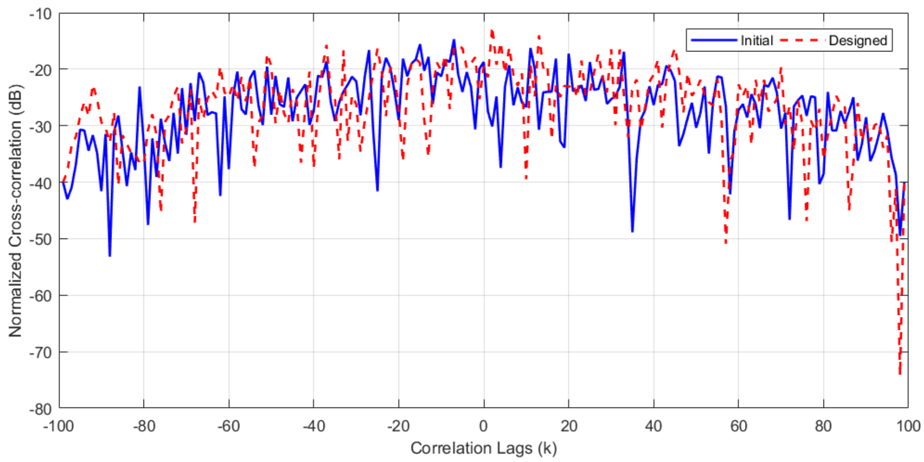

Figure 4.14 Initial and final cross-correlations of first and third designed sequences

In addition to cross-correlations, we also examine autocorrelations of the designed sequences. Figures 4.16, 4.17, and 4.18 display autocorrelations of the first, second, and third designed sequences, respectively. As a consequence of a rather high λ value, temporal suppression is of secondary importance in the MIMO SCAN algorithm. Hence, spectral suppression is more pronounced than temporal suppression.

Table 4.2 displays the performance metrics of the initial and final sequences designed by MIMO SCAN algorithm for $\lambda = 0.8$. Similar to the previous simulation example, MIMO SCAN algorithm provides suppression of autocorrelation sidelobes

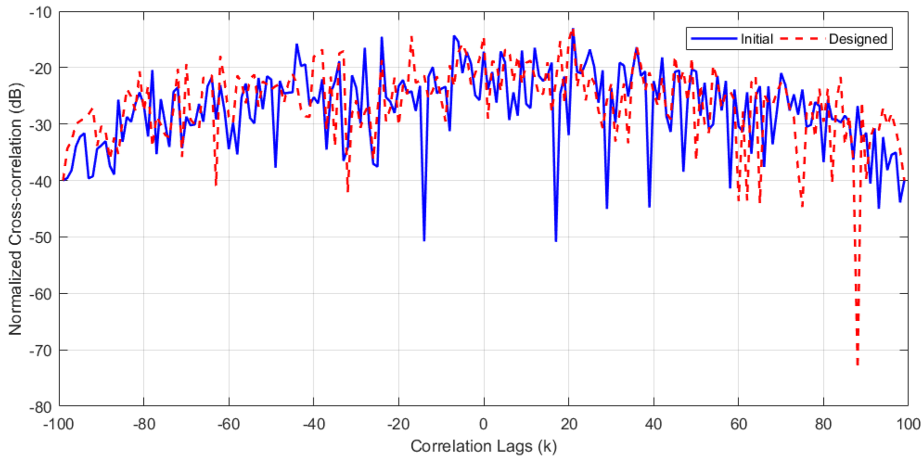

Figure 4.15 Initial and final cross-correlations of second and third designed sequences

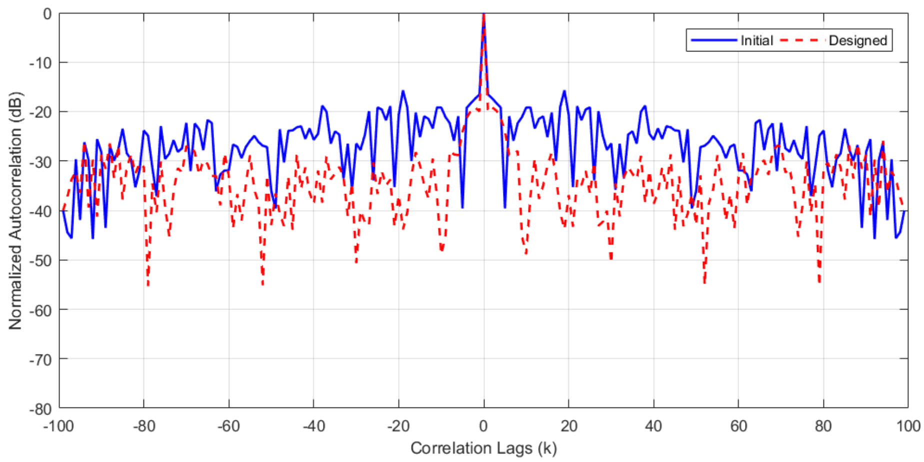

Figure 4.16 Initial and final autocorrelations of the first designed sequence

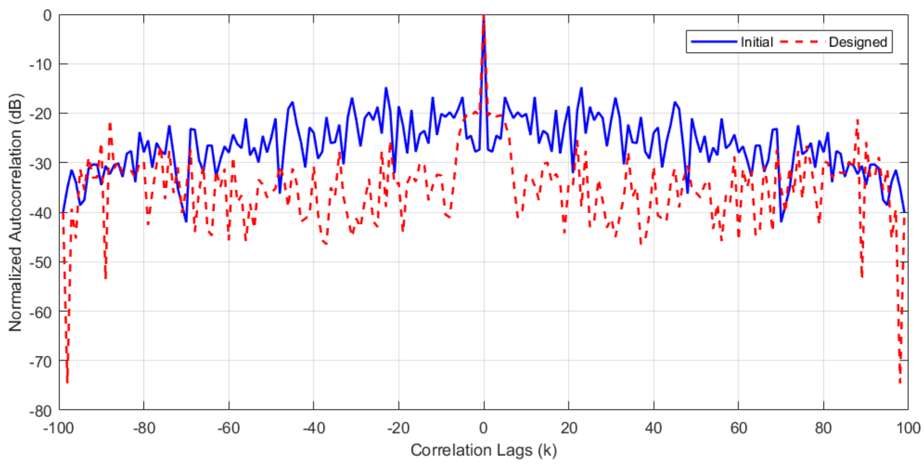

Figure 4.17 Initial and final autocorrelations of the second designed sequence

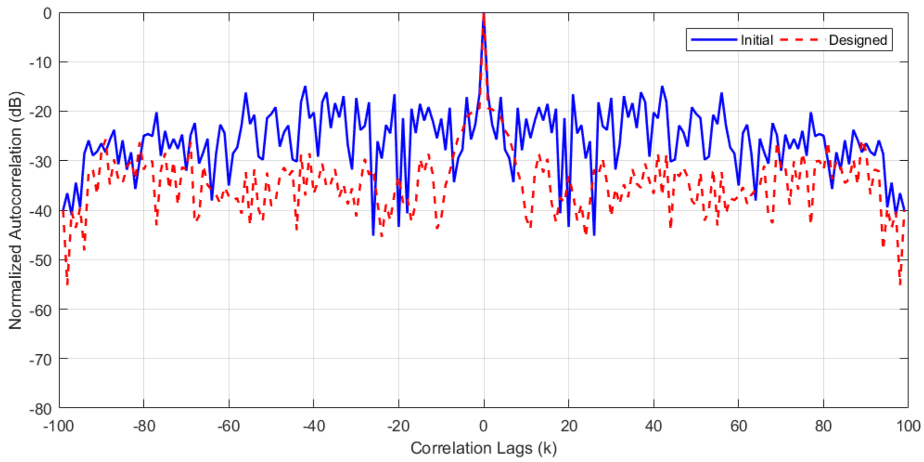

Figure 4.18 Initial and final autocorrelations of the third designed sequence

Table 4.2 Performance metrics of MIMO SCAN having three radar sequences

MIMO SCAN	ISL	MF	Stopband Level (dB)
Initial 1^{st} Sequence	8.5385e+03	1.1712	-4.1152
Initial 2^{nd} Sequence	8.8345e+03	1.1319	-1.1418
Initial 3^{rd} Sequence	1.0856e+04	0.9211	-3.1459
Final 1^{st} Sequence	1.9630e+03	5.0943	-13.5619
Final 2^{nd} Sequence	2.0149e+03	4.9630	-13.7411
Final 3^{rd} Sequence	1.8635e+03	5.3663	-13.8912

as indicated by the decreased ISL values for all three designed sequences. In parallel, the MF values of designed sequences are increased as expected. By virtue of high weighting parameter value ($\lambda = 0.8$), stopband levels for the designed sequences are considerably reduced over the predetermined stopband.

4.2 Simulation Examples for MIMO SHAPE

In the first example, we take the sequence length as $N = 100$ and the number of designed sequences as $M = 2$. Except for the notch, the spectral upper bound, $\mathbf{u}$, is merely applied to force the spectrum below 0 dB across the whole frequency range. Over the stopband, $\Omega = [0.65, 0.8)$, the designed spectrum is forced to be under -40

dB. No spectral lower bound, **l**, is applied in the first example. The FFT size is taken to be $\tilde{N} = 1000$ and the number of iterations is fixed as 2×10^5. The spectra of the resultant designed sequences can be seen in Figures 4.19 and 4.20, respectively, where the employed spectral upper bound is shown using a green line. As can be seen in Figures 4.19 and 4.20, the spectra of both designed sequences contain the desired notch of -40 dB as specified by the employed spectral upper bound. It is interesting to see from Figure 4.21 that the CESD of the designed sequences contains a deeper notch of -60 dB although it does not obey the spectral upper bound at other frequency values. Finally, cross-correlation sidelobes of the designed sequences remain quite low as seen in Figure 4.22 providing near orthogonality of the designed sequences. Furthermore, sidelobes of the autocorrelations of both designed sequences are not suppressed as indicated in Figures 4.23 and 4.24. This is no surprise because the MIMO SHAPE algorithm does not employ temporal constraints.

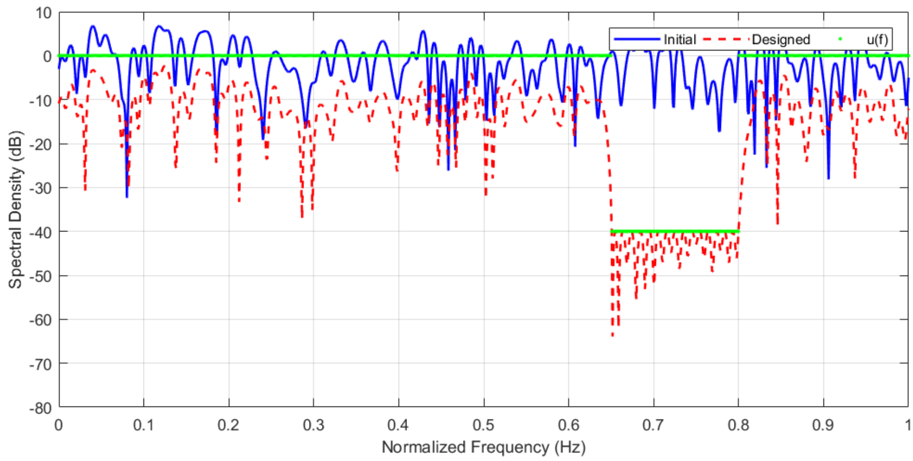

Figure 4.19 Initial and final spectra of the first designed sequence

Table 4.3 displays the performance metric values of the initial and final designed sequences by MIMO SHAPE algorithm. Notice that ISL values of the sequences designed by MIMO SHAPE algorithm are worse than the ISL values of initial sequences. This is because the SHAPE algorithm constrains only the spectra of designed sequences but not their autocorrelations. MF values of the initial and final designed sequences are given in the third column of Table 4.3. Similar to ISL values, MF values of the designed sequences via MIMO SHAPE are worse than that of initial sequences.

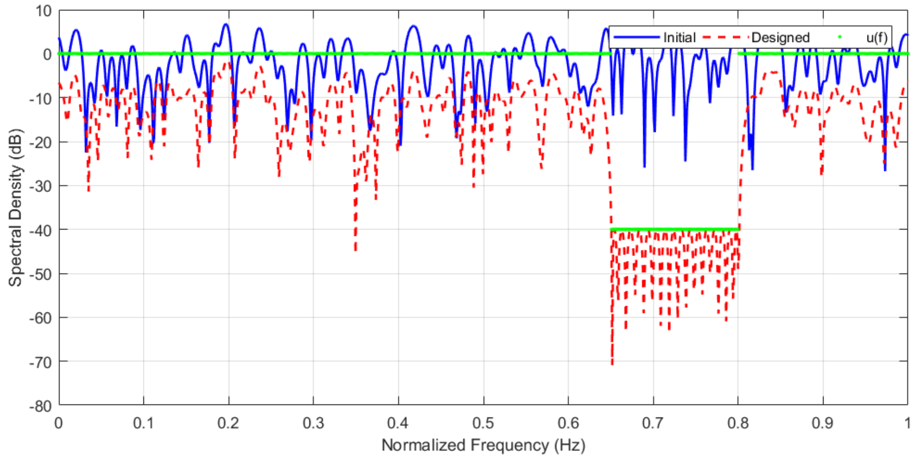

Figure 4.20 Initial and final spectra of the second designed sequence

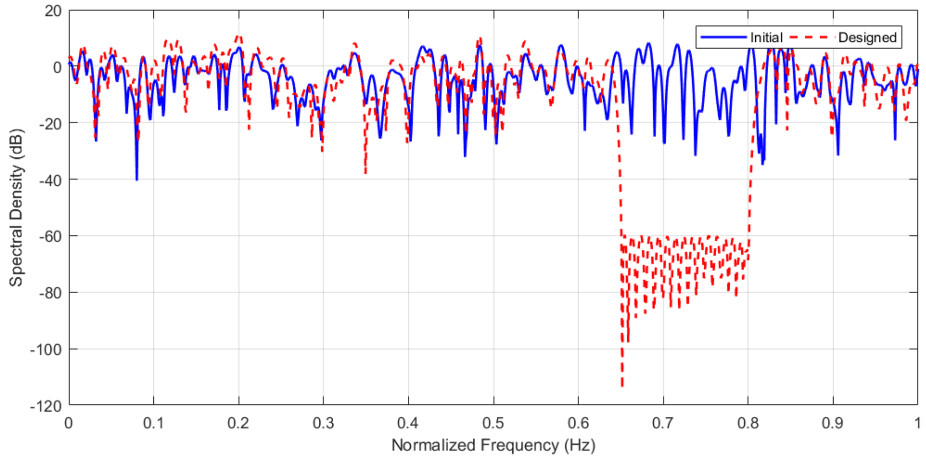

Figure 4.21 CESDs of initial and final designed sequences

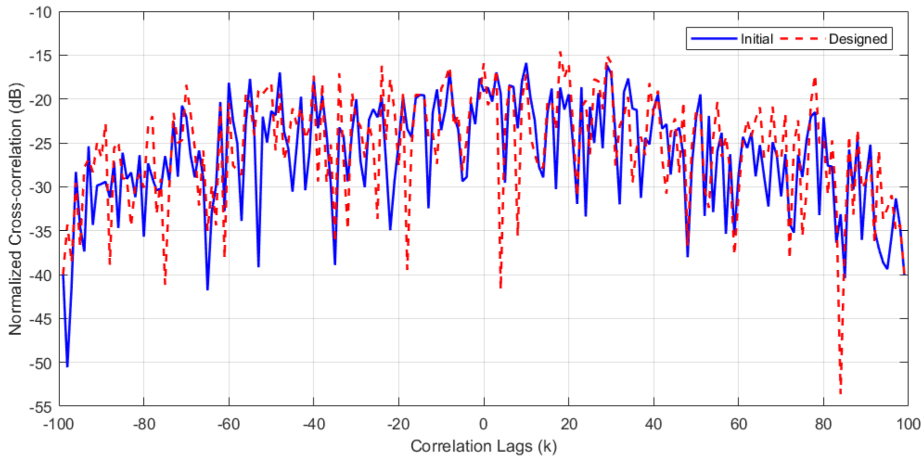

Figure 4.22 Cross-correlations of initial and final designed sequences

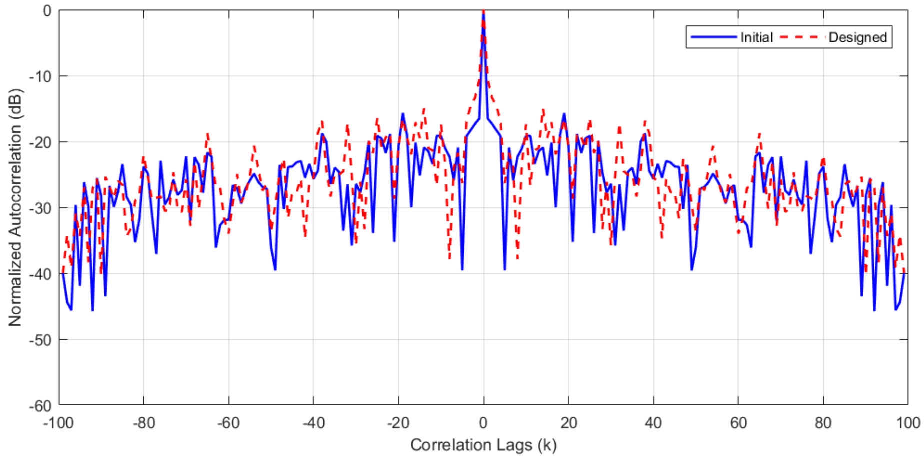

Figure 4.23 Initial and final autocorrelations of the first designed sequence

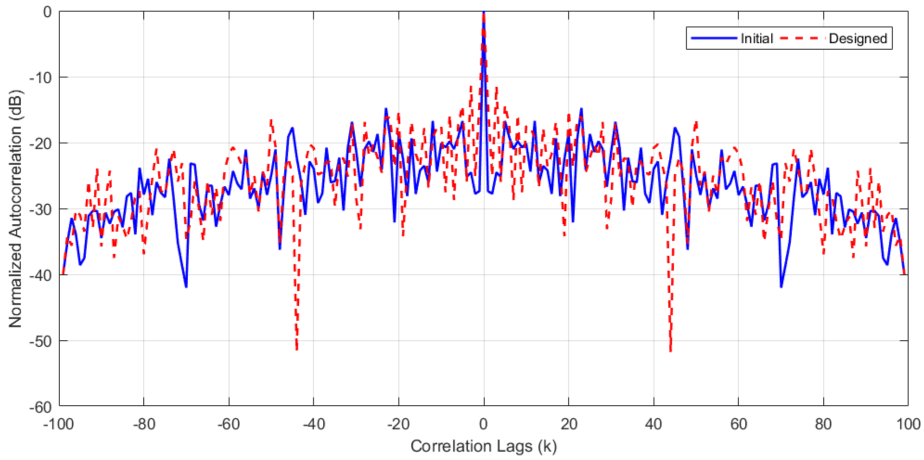

Figure 4.24 Initial and final autocorrelations of the second designed sequence

Table 4.3 Performance metrics of MIMO SHAPE having two radar sequences

MIMO SHAPE	ISL	MF	Stopband Level (dB)
Initial 1^{st} Sequence	8.538e+03	1.1712	-3.1252
Initial 2^{nd} Sequence	8.834e+03	1.1319	-2.2628
Final 1^{st} Sequence	1.2554e+04	0.7966	-43.3248
Final 2^{nd} Sequence	1.3386e+04	0.7470	-45.2132

Average stopband levels are presented in the fourth column of Table 4.3. Based on the much lower stopband levels obtained by MIMO SHAPE, we can conclude that spectral performance of MIMO SHAPE is much better than that of MIMO SCAN. This is no surprise because, by design, the SHAPE algorithm solely constrains the spectrum and is not concerned with autocorrelation sidelobes.

In the second simulation example, we employ a matrix of $N \times M$ where $N = 100$ and $M = 3$ for designing three unimodular sequences with the length of 100. When iterations terminate, the MIMO SHAPE algorithm generates the final designed sequences. The spectral notch is placed in the normalized frequency band $\Omega = [0.75, 0.85)$. Figures 4.25, 4.26, and 4.27 show the initial and final spectra of the designed sequences.

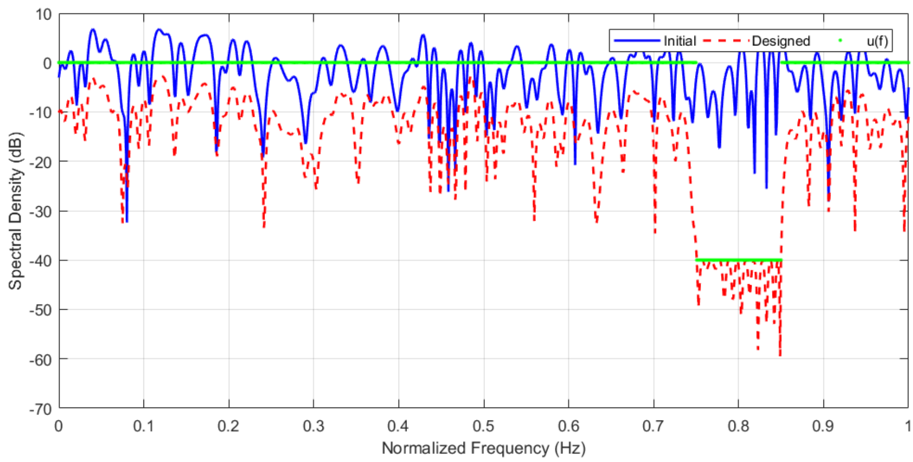

Figure 4.25 Initial and final spectra of the first designed sequence

CESDs of initial and final designed sequences are shown in Figures 4.28, 4.29, and

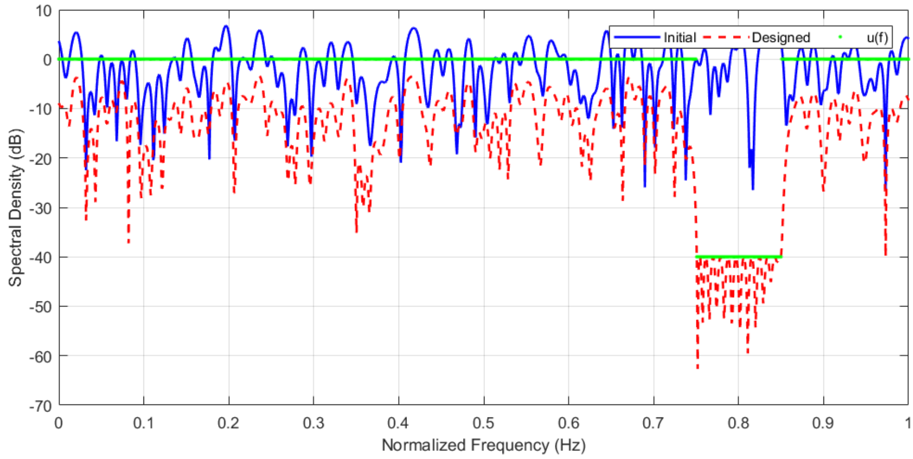

Figure 4.26 Initial and final spectra of the second designed sequence

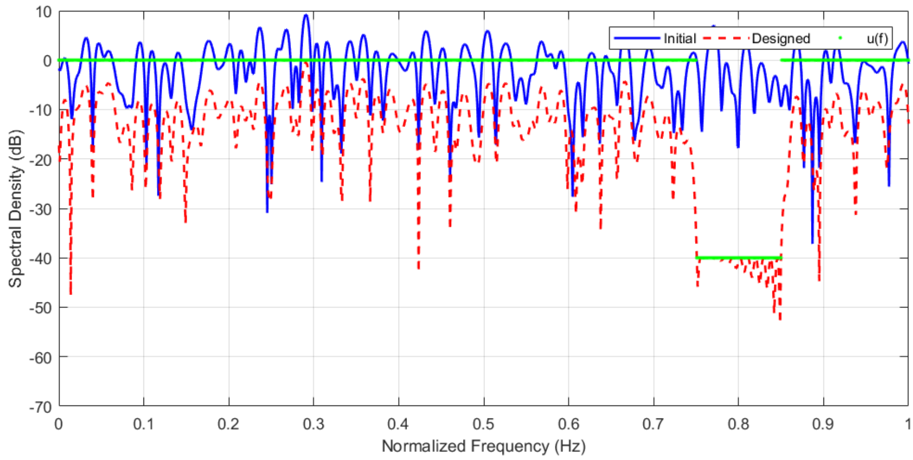

Figure 4.27 Initial and final spectra of the third designed sequence

4.30 for the first and second designed sequences, the first and third designed sequences, and the second and third designed sequences, respectively. Spectral suppression over stopband frequencies is close to −60 dB for all three CESDs, indicating the effectiveness of the MIMO SHAPE algorithm in suppressing desired frequency bands.

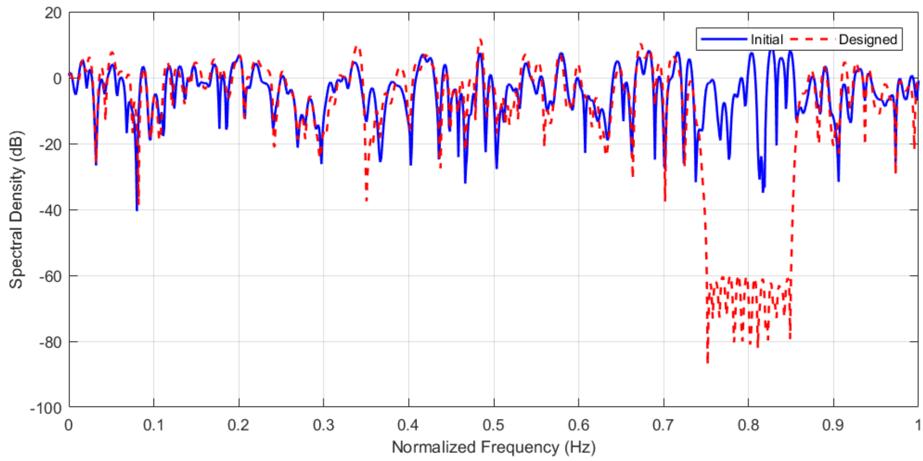

Figure 4.28 The initial and final CESDs of the first and second designed sequences

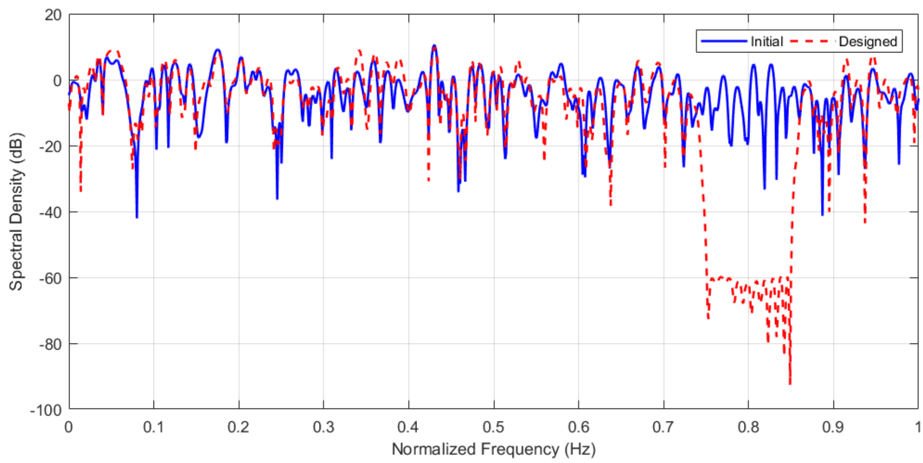

Figure 4.29 The initial and final CESDs of the first and third designed sequences

To observe the mutual relationship of designed sequences in pairs of two, we can look at their cross-correlations. Figures 4.31, 4.32, and 4.33 display cross-correlations of the inital and final sequences for the first and second designed sequences, the first and third designed sequences, and the second and third designed sequences, respectively.

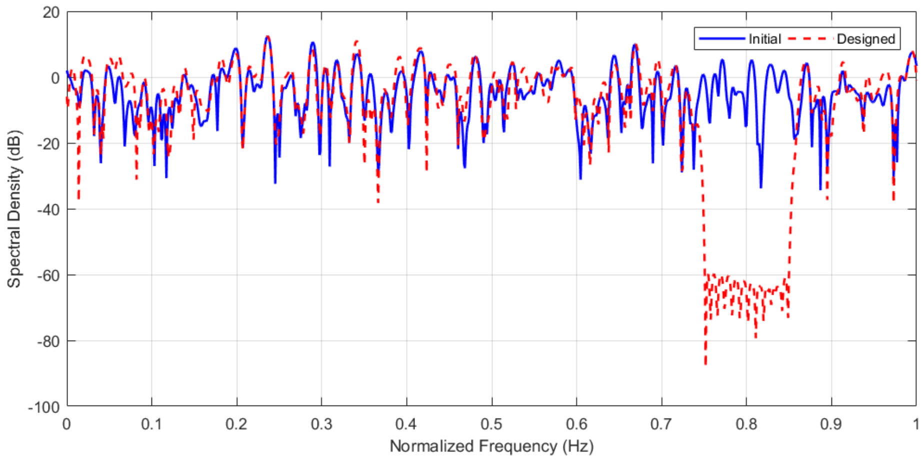

Figure 4.30 The initial and final CESDs of the second and third designed sequences

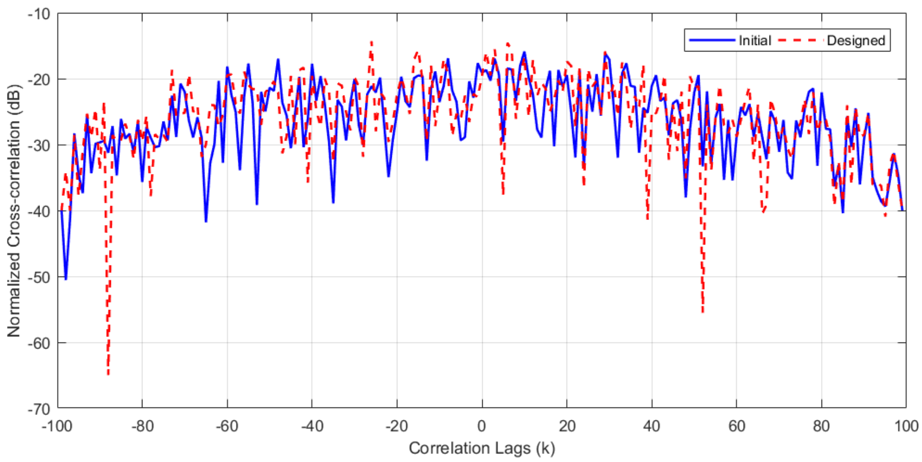

Figure 4.31 Initial and final cross-correlations of the first and second designed sequences

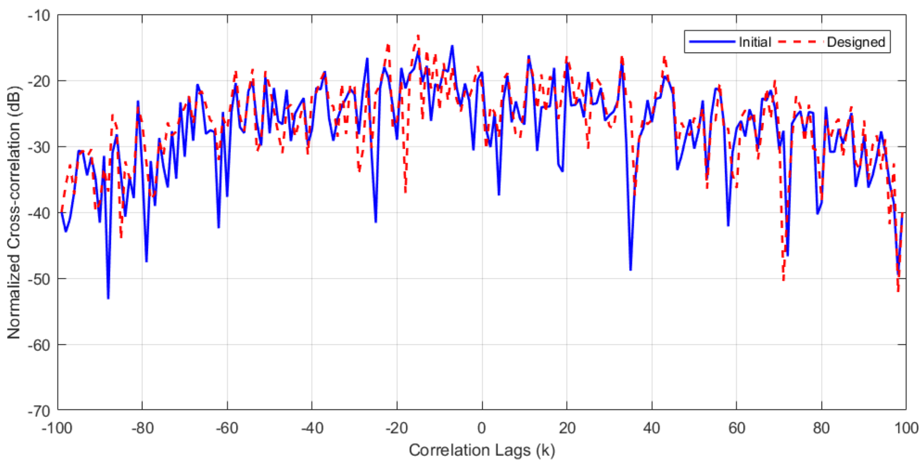

Figure 4.32 Initial and final cross-correlations of the first and third designed sequences

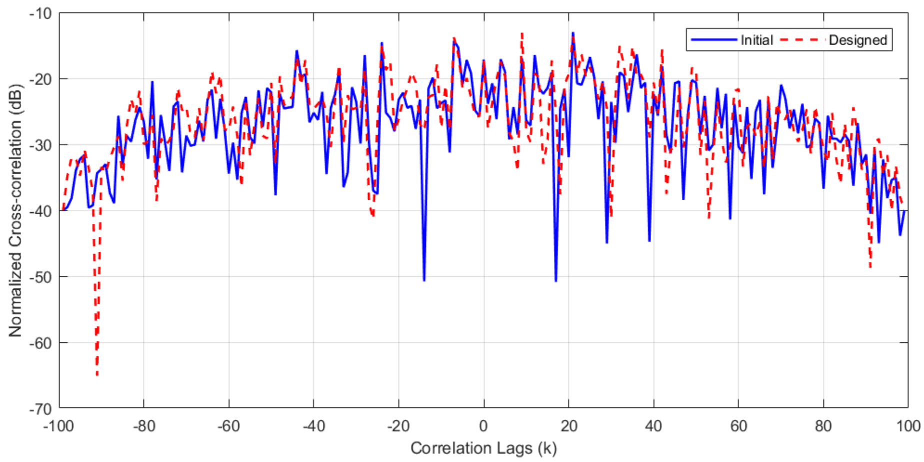

Figure 4.33 Initial and final cross-correlations of the second and third designed sequences

Table 4.4 Performance metrics of MIMO SHAPE having three radar sequences

MIMO SHAPE	ISL	MF	Stopband Level (dB)
Initial 1^{st} Sequence	8.5385e+03	1.1712	-4.1152
Initial 2^{nd} Sequence	8.8345e+03	1.1319	-1.1418
Initial 3^{rd} Sequence	1.0856e+04	0.9211	-3.1459
Final 1^{st} Sequence	1.1471e+04	0.8717	-43.2971
Final 2^{nd} Sequence	1.0823e+04	0.9239	-43.9944
Final 3^{rd} Sequence	1.2754e+04	0.7841	-41.5524

Table 4.4 displays the performance metric values of the initial and final designed sequences by MIMO SHAPE algorithm. Similar to the preceding simulation example, MIMO SHAPE algorithm does not provide any improvement in temporal domain as indicated by the increased ISL values for all three designed sequences. In parallel to increased ISL values, the MF values for designed sequences are decreased compared to the initial sequences. On the other hand, its performance in terms of spectral suppression is much better than MIMO SCAN algorithm.

4.3 Simulation Example for MIMO SHAPE with Lower Bound

In this section, we investigate the effect of employing a lower bound in the MIMO SHAPE algorithm together with an upper bound. In this example, the stopband is assigned as $\Omega = [0.375, 0.425)$ in normalized frequency. The upper bound is taken as 0 dB over the passband and -30 dB over the stopband. Alongside the upper bound, the lower bound is specified as -10 dB over the passband and -40 dB over the stopband. The length of designed sequences is $N = 100$ and the number of designed sequences is $M = 2$. In this simulation example, the iteration number is set as 2×10^5. By employing the lower bound together with the upper bound, the spectra of the designed sequences are forced to stay in a restricted region as seen in Figures 4.34 and 4.35 which, respectively, show the spectra of the first and second designed sequences. CESD and cross-correlation of the designed sequences can be seen in Figures 4.36 and 4.37, respectively. Finally, autocorrelations of designed sequences are shown in Figures 4.38 and 4.39.

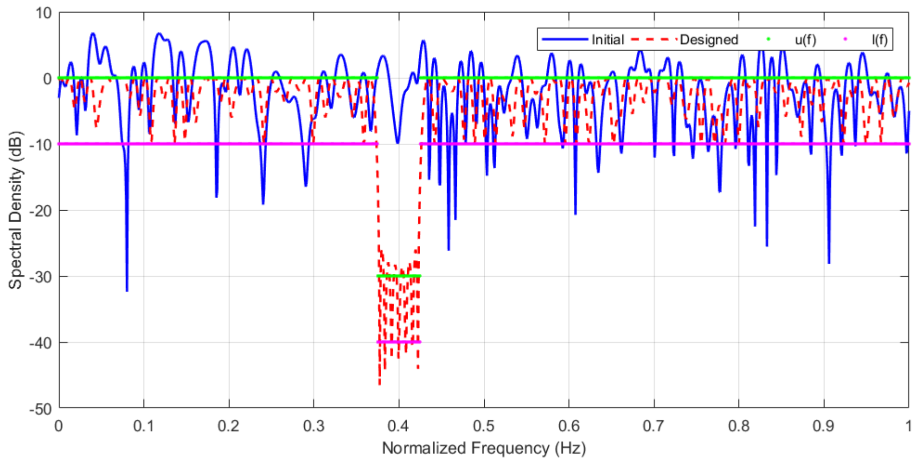

Figure 4.34 Initial and final spectra of the first designed sequence

4.4 Generating OFDM Signals via MIMO SHAPE Algorithm

Other than generating radar transmit signals with suppressed stopbands, the MIMO SHAPE algorithm can also be utilized for forming communication signals

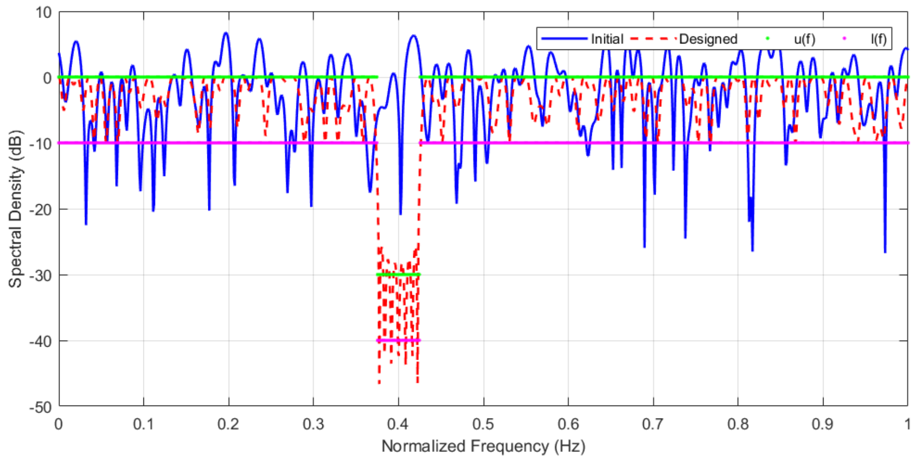

Figure 4.35 Initial and final spectra of the second designed sequence

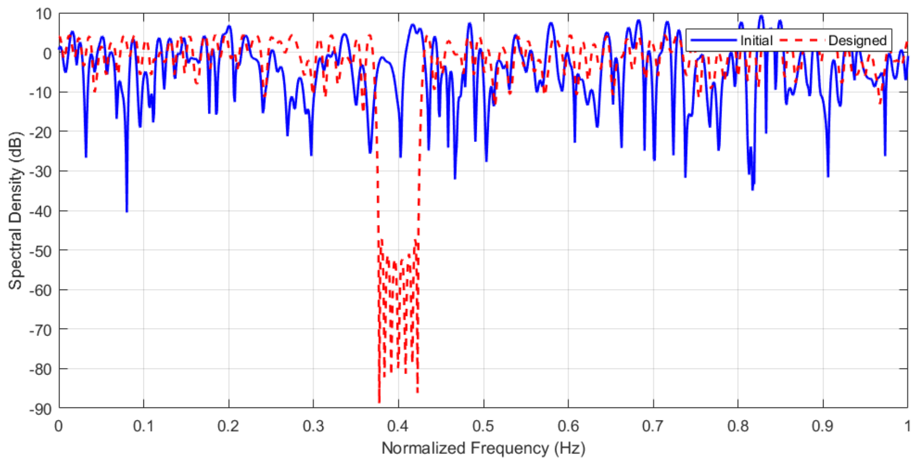

Figure 4.36 CESDs of initial and final designed sequences

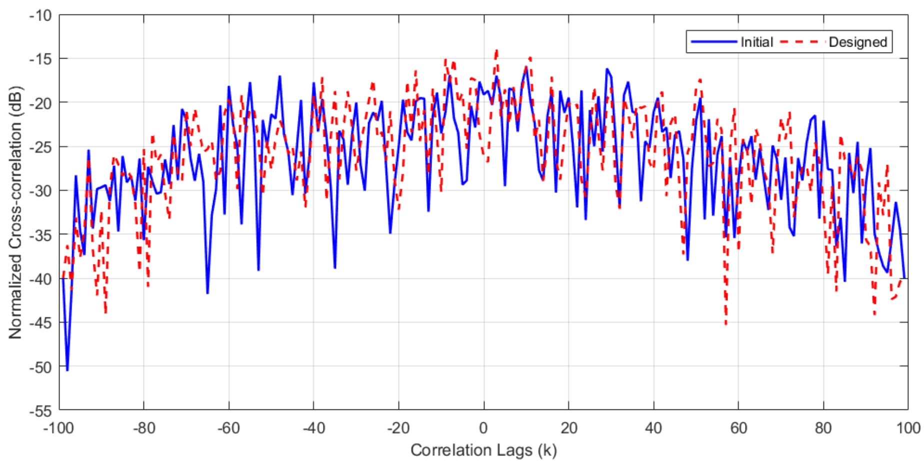

Figure 4.37 Cross-correlations of initial and final designed sequences

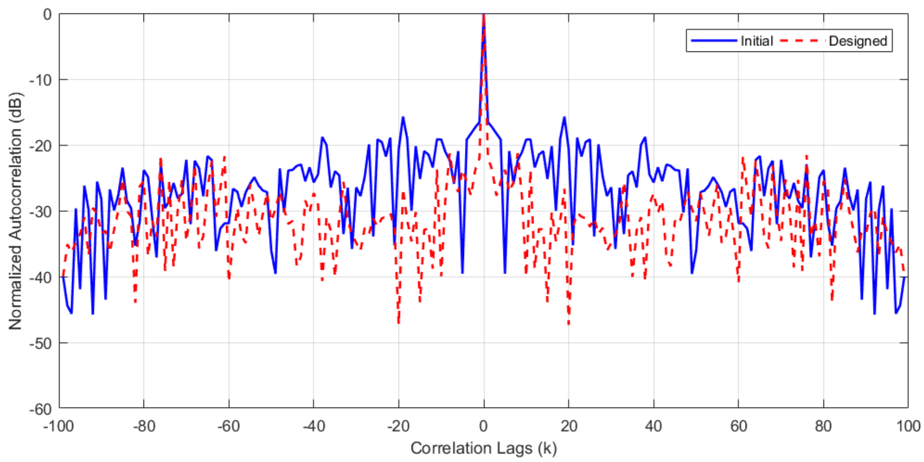

Figure 4.38 Initial and final autocorrelations of the first designed sequence

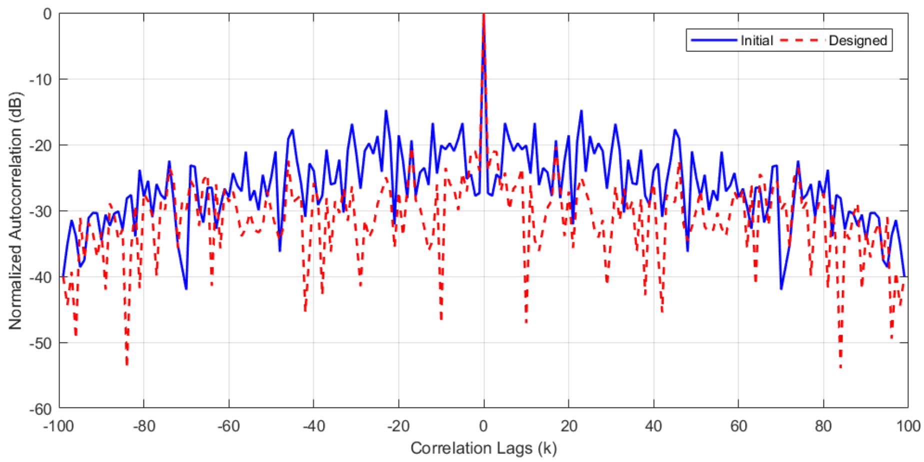

Figure 4.39 Initial and final autocorrelations of the second designed sequence

such as orthogonal frequency division multiplexing (OFDM) signals which have specially designed spectra (Clancy & Walker, 2006). In this section, we also utilize the MIMO SHAPE algorithm for designing a sample OFDM signal. In this simulation example, we design two OFDM signals ($M = 2$) having spectra with a triangularly shaped passband by employing unimodular sequences with length $N = 100$. The triangular passband is placed at $\Omega = [0.35, 0.55)$ in normalized frequencies. The upper bound at the passband starts with 0 dB at the left edge and ends with -30 dB at the right edge of the passband. The lower bound, which also has a triangular shape over the passband, starts with -10 dB at the left edge and ends with -40 dB value at the right edge of the passband. At other frequencies, the upper and lower bounds are assigned as -30 dB and -40 dB, respectively. The DFT size is chosen as 10^3 and the number of iterations is set to be 2×10^5. As can be seen in Figures 4.40 and 4.41, spectra of both designed sequences follow the triangular bounds at passband. Interestingly, the CESD of both designed sequences plotted in Figure 4.42 also takes the triangular shape over the passband. Cross-correlation of designed sequences does not seem to provide near orthogonality as can be seen in Figure 4.43. Furthermore, autocorrelations of both designed sequences have worse sidelobe characteristic than their initial autocorrelations as shown in Figures 4.44 and 4.45. Again, this is a result of the fact that MIMO SHAPE algorithm does not constrain autocorrelation of the temporal domain.

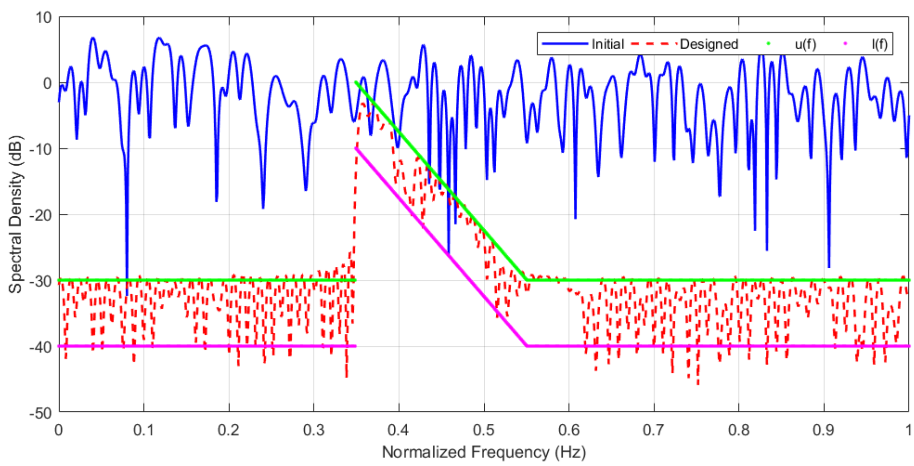

Figure 4.40 Initial and final spectra of the first designed sequence

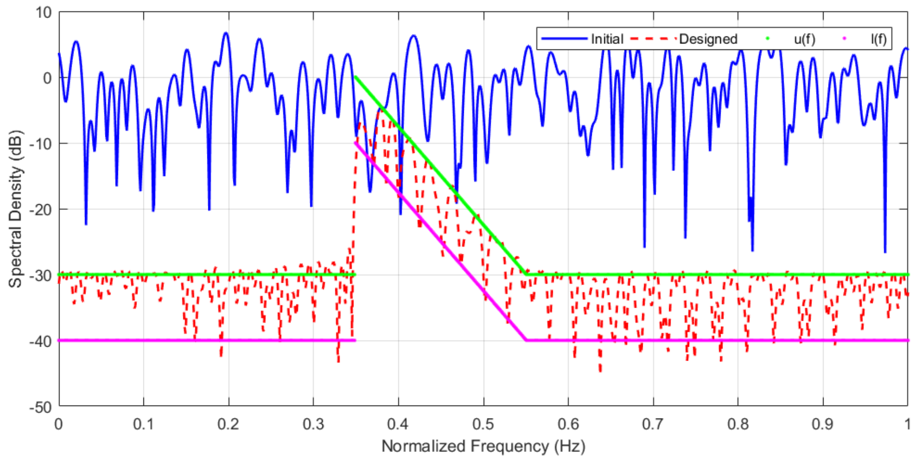

Figure 4.41 Initial and final spectra of the second designed sequence

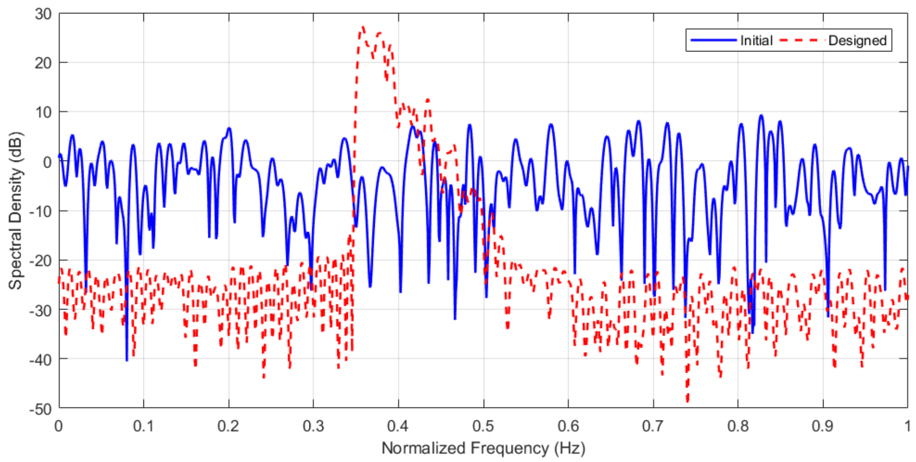

Figure 4.42 CESDs of initial and final designed sequences

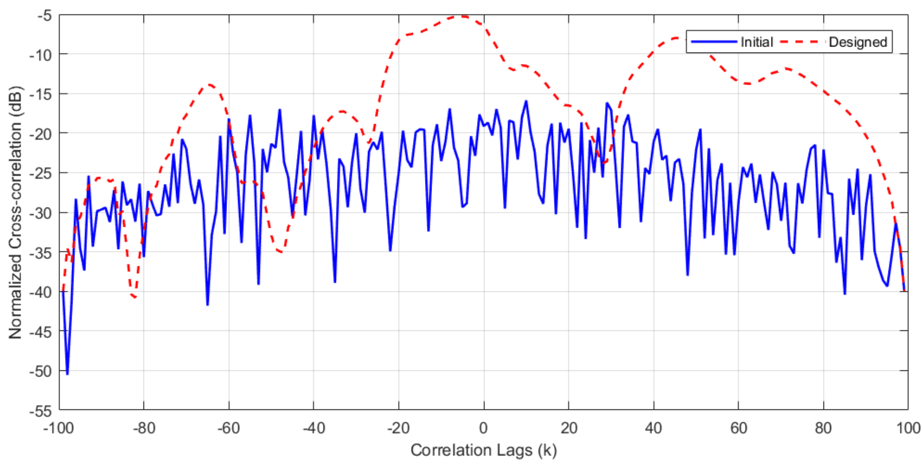

Figure 4.43 Cross-correlations of initial and final designed sequences

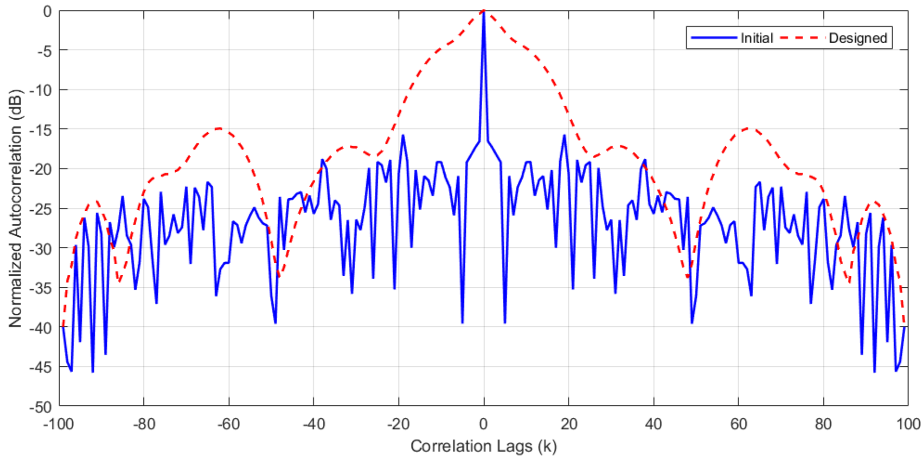

Figure 4.44 Initial and final autocorrelations of the first designed sequence

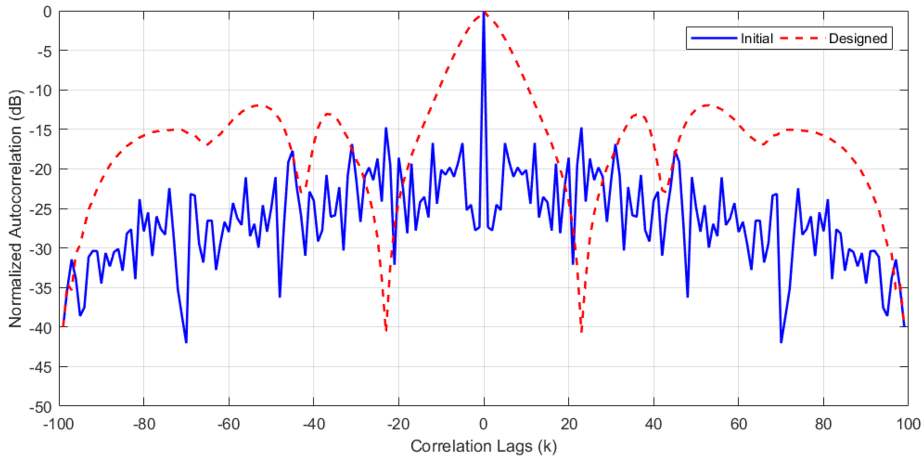

Figure 4.45 Initial and final autocorrelations of the second designed sequence

4.5 Application of SCAN and SHAPE Algorithms Successively in a Combined Fashion

When the spectra of sequences designed by SCAN algorithm are examined, it can be seen that there are fluctuations both in the passband and the stopband. Similarly, if we observe the spectra of sequences designed by the SHAPE algorithm, when the lower bound is not employed along with the upper bound, there exist fluctuations below the upper bound. However, the SHAPE algorithm can inherently manage forming flat passbands or stopbands. To reduce fluctuations, we propose an application where the SCAN and SHAPE algorithms are applied in succession.

In this simulation example, the SCAN algorithm is initialized by a unimodular sequence of length $N = 100$. The weighting factor is assigned as $\lambda = 0.8$. A spectral notch at the frequency band $\Omega = [0.35, 0.45)$ is placed. The initial and designed spectra are shown in Figure 4.46. We can notice that there are fluctuations both in the passband and stopband of the spectrum of the designed sequence.

After the SCAN algorithm is terminated, the resultant designed sequence is utilized to initialize the SHAPE algorithm for which an upper bound of -10 dB at passband frequencies and of -30 dB at stopband frequencies is employed. The DFT size is chosen as 10^3 and the number of iterations is assigned as 2×10^5. In Figure 4.47, the resultant spectrum of the SHAPE algorithm is plotted together with the initial spectrum which was obtained by the SCAN algorithm. In Figure 4.48, autocorrelation of the initial sequence, autocorrelation of the designed sequence by SCAN, and autocorrelation of the final designed sequence by the SHAPE algorithm are plotted together.

4.6 Computational Complexities of MIMO SCAN and MIMO SHAPE

In this section, we investigate the computational complexities of MIMO SCAN and MIMO SHAPE algorithms. Table 4.5 shows the computation time (in seconds) of

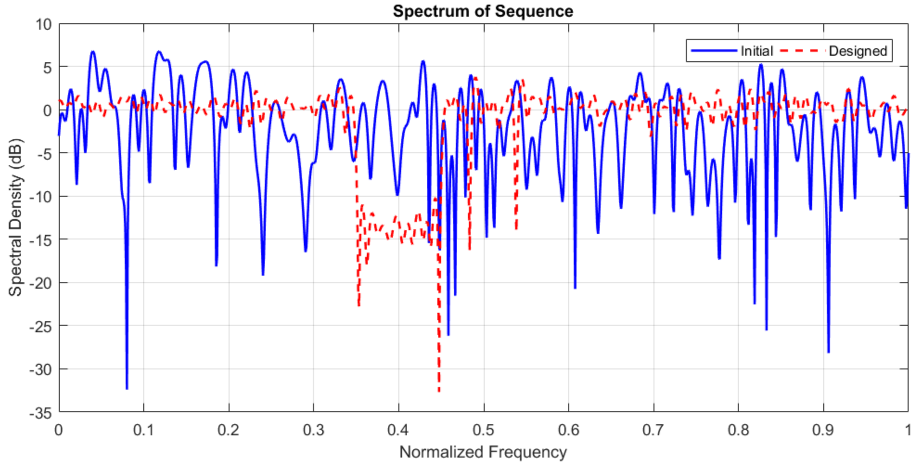

Figure 4.46 Initial and designed spectra by the SCAN algorithm

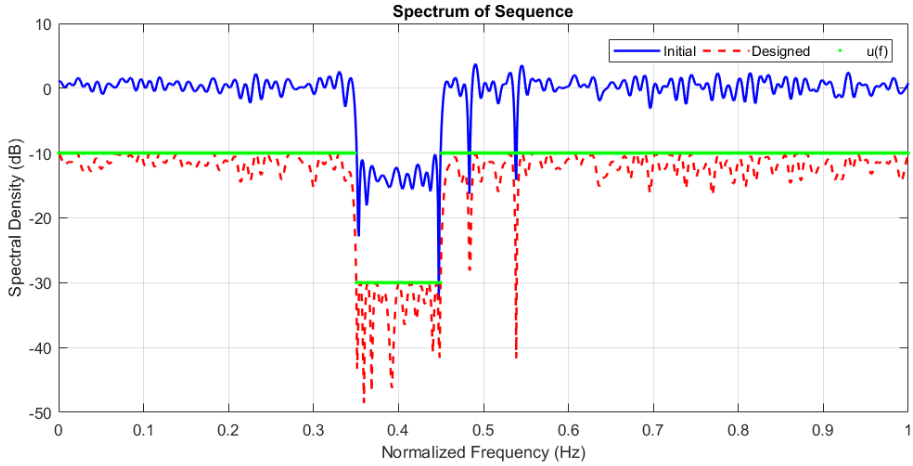

Figure 4.47 Initial spectrum by the SCAN algorithm and the designed spectrum by the SHAPE algorithm

Figure 4.48 Autocorrelations of the initial sequence, designed sequence by SCAN (Designed 1), and the final designed sequence by the SHAPE algorithm (Designed 2)

Table 4.5 Computational complexities of MIMO SCAN and MIMO SHAPE algorithms for $M = 2$ and $M = 3$

	M=2	M=3
MIMO SCAN	811.25 sec	996.82 sec
MIMO SHAPE	78.66 sec	103.40 sec

MIMO SCAN and MIMO SHAPE algorithms for $M = 2$ and $M = 3$. All the simulations were performed on a i7-7500U PC with 16 GB memory and 2.9 GHz processor speed. We employed unimodular sequences of length $N = 100$. The FFT size was assigned as $\tilde{N} = 1000$ and the number of iterations was set as 2×10^5. The MIMO SCAN algorithm takes 811.25 seconds and 996.82 seconds, respectively, for $M = 2$ and $M = 3$. The required time of MIMO SHAPE algorithm, on the other hand, for $M = 2$ and $M = 3$ are 78.66 seconds and 103.40 seconds, respectively. Thus, MIMO SCAN requires almost ten times more time than the MIMO SHAPE algorithm. The reason for that increase is that, different from the MIMO SHAPE algorithm, MIMO SCAN tries to suppress autocorrelation sidelobes as an additional temporal constraint.

CHAPTER FIVE
CONCLUSION

In this thesis, we have proposed extensions of the radar waveform design methods of SCAN and SHAPE for MIMO systems. We first reviewed the SISO SCAN and SHAPE algorithms along with simulation examples indicating their characteristics and properties. We also compared those two algorithms in terms of their advantages and disadvantages. The SCAN algorithm provides improvements in both temporal and spectral domains by employing a weighting parameter which trades off temporal suppression against spectral suppression. Different from the SCAN algorithm, the SHAPE algorithm provides only spectral suppression by introducing upper and lower spectral bounds.

We then defined MIMO extensions of SCAN and SHAPE algorithms. We presented the implementation steps of MIMO SCAN and MIMO SHAPE algorithms. As for generalization of the SCAN and SHAPE algorithms to MIMO radar systems, one important consideration is to decide whether to include the same passband and stopband for each sequence. Another consideration in implementing MIMO SCAN algorithm is to determine whether the weighting factor should be selected as variable or fixed.

After extending SCAN and SHAPE algorithms to MIMO radar systems, we presented some simulation examples. We performed simulation examples of both MIMO algorithms for the cases of two and three unimodular sequences. During the simulation examples, we measured some performance metrics such as ISL, MF, and spectral suppression level at stopbands (in dB).

Finally, we note that the number of designed sequences can be increased straightforwardly. That is why, we demonstrated the case of including three different unimodular sequences. In this case, initial and designed final cross-correlations and CESDs were shown for two different designed sequences from the set of three sequences. Both MIMO SCAN and MIMO SHAPE algorithms are able to design mutually orthogonal transmit sequences with low-level cross-correlations.

MIMO SHAPE algorithm was applied for designing communication signals as well. We demonstrated that MIMO SHAPE algorithm could generate OFDM signals with a certain spectral shape. Although the designed sequences possessed desired spectral shape, temporal suppression could not be obtained as a shortcoming of SHAPE algorithm.

For future work, application of alternative optimization methods such as majorization-minimization could be considered for designing MIMO radar transmit signals.

REFERENCES

Alessio, S. M. (2015). *Digital Signal Processing and Spectral Analysis for Scientists: Concepts and Applications*. Signals and Communication Technology, Springer International Publishing.

Aubry, A., Carotenuto, V., & Maio, A. D. (2016). Forcing multiple spectral compatibility constraints in radar waveforms. *IEEE Signal Processing Letters*, *23*(4), 483–487.

Bliss, D., & Forsythe, K. (2003). Multiple-input multiple-output (MIMO) radar and imaging: Degrees of freedom and resolution. In *Conference Record of the Asilomar Conference on Signals, Systems and Computers*.

Clancy, C. T., & Walker, B. (2006). Spectrum shaping for interference management in cognitive radio networks. *SDR Forum Technical Conference*, (11).

Cook, M. R., Higgins, T., & Shackelford, A. K. (2010). Thinned spectrum radar waveforms. In *2010 International Waveform Diversity and Design Conference, WDD 2010*.

Fishler, E., Haimovich, A., Blum, R. S., Cimini, L. J., Chizhik, D., & Valenzuela, R. A. (2006). Spatial diversity in radars - Models and detection performance. *IEEE Transactions on Signal Processing*, *54*.

Haykin, S. (2007). Cognitive Radar. In *Knowledge-Based Radar Detection, Tracking, and Classification* (1st ed.)(9-30), John Wiley & Sons, Inc.

He, H., Li, J., & Stoica, P. (2012). *Waveform design for active sensing systems: A computational approach* (1st ed.) . Cambridge University Press.

He, H., Stoica, P., & Li, J. (2009). Designing unimodular sequence sets with good correlations - Including an application to MIMO radar. *IEEE Transactions on Signal Processing*, *57*(11), 4391–4405.

He, H., Stoica, P., & Li, J. (2010). Waveform design with stopband and correlation constraints for cognitive radar. *2010 2nd International Workshop on Cognitive Information Processing, CIP2010*, *1*(1), 344–349.

Levanon, N., & Mozeson, E. (2004). *Radar Signals*. John Wiley & Sons, Inc.

Li, J., Stoica, P., Xu, L., & Roberts, W. (2007). On Parameter Identifiability of MIMO Radar. *IEEE Signal Processing Letters*, *14*(12), 968–971.

Liang, J., So, H. C., Leung, C. S., Li, J., & Farina, A. (2015). Waveform Design With Unit Modulus and Spectral Shape Constraints via Lagrange Programming Neural Network. *IEEE Journal on Selected Topics in Signal Processing*, *9*(8), 1377–1386.

Lindenfeld, M. J. (2004). Sparse frequency transmit and receive waveform design. *IEEE Transactions on Aerospace and Electronic Systems*, 851–861.

Patton, L. K., Bryant, C. A., & Himed, B. (2012). Radar-centric design of waveforms with disjoint spectral support. *IEEE National Radar Conference - Proceedings*, (1), 0269–0274.

Petrolati, D., Angeletti, P., & Toso, G. (2012). New piecewise linear polyphase sequences based on a spectral domain synthesis. *IEEE Transactions on Information Theory*, *58*(7), 4890–4898.

Rowe, W., Stoica, P., & Li, J. (2014). Spectrally constrained waveform design. *IEEE Signal Processing Magazine*, 157–162.

Sebt, M. A., Norouzi, Y., Sheikhi, A., & Nayebi, M. M. (2008). OFDM radar signal design with optimized Ambiguity Function. *2008 IEEE Radar Conference*.

Song, J., Babu, P., & Palomar, D. P. (2015). Optimization methods for sequence design with low autocorrelation sidelobes. *ICASSP, IEEE International Conference on Acoustics, Speech and Signal Processing - Proceedings*, *2015-Augus*(15), 3033–3037.

Stoica, P., He, H., & Li, J. (2009). New algorithms for designing unimodular sequences with good correlation properties. *IEEE Transactions on Signal Processing*, *57*, 1415–1425.

Wang, G., & Lu, Y. (2010). Sparse frequency waveform design for MIMO radar. *Progress In Electromagnetics Research B*, *20*, 19–32.

Wang, G., & Lu, Y. (2011). Designing single/multiple sparse frequency waveforms with sidelobe constraint. *IET Radar, Sonar & Navigation*, *5*(1), 32–38.

Xu, L., Li, J., & Stoica, P. (2008). Target detection and parameter estimation for MIMO radar systems. *IEEE Transactions on Aerospace and Electronic Systems*, *44*.

APPENDIX
COMPUTER PROGRAMS

Computer Program of MIMO SCAN

```
function outM = FX_mimoSCAN(intM,LNFFT,Lambda,MAXIT,StopBand)
% Construction of G matrix given stopband criterion
% Ntilde*Ntilde DFT matrix construction
FNT=FXFmatrix(LNFFT);
[RowStop, ColumnStop]=size(StopBand);
% Nullfying stopband samples
for k=1:RowStop
    FNT(:,StopBand(k,1):StopBand(k,ColumnStop))=0;
end
% G matrix elements
GMat=FNT;
GMat(:, ~any(GMat,1))=[];
[RowX, ColumnX]=size(intM); LN2=2*RowX;
Amat=FXAmatrixN(intM);
AmatH=ctranspose(Amat);
LCP=1;
while LCP <= MAXIT
    %-----Spectral-----
    XTil=[intM ; zeros((LNFFT-RowX),ColumnX)];
    Alpha=ctranspose(GMat)*XTil;
    inverseAlpha=GMat*Alpha;
    CP1=inverseAlpha(1:RowX,:);
    %-----Correlation-----
    Xzerop=[intM; zeros(RowX,ColumnX)];
    fftXzerop=(AmatH*Xzerop)/(sqrt(LN2));
    XzeropPhase=angle(fftXzerop);
    VMatrix=exp(1j*XzeropPhase)/sqrt(2);
    ifftVMatrix=ifft(VMatrix)*sqrt(LN2);
    CP2=ifftVMatrix(1:RowX,:);
    %-----Phase Determination-----
    PhaseTemp=angle(Lambda*CP1 + (1-Lambda)*CP2);
    TempoutX=exp(1j*PhaseTemp);
```

```
        intM=TempoutX;
        LCP=LCP+1;
end
outM=intM;
end
```

Computer Program of MIMO SHAPE

```
function [outS ,BP]=FX_mimoSHAPE(intM ,UPLM,LOWLM, Window ,MAXIT,NFFT)
[RowX , ColumnX]=size(intM);
BTM=real(ones(NFFT,ColumnX));
ZXM=zeros(NFFT,ColumnX);
AFT=1/sqrt(NFFT);
Xzerop=[intM ; zeros((NFFT-RowX),ColumnX)];
fftXzerop=AFT*(fft(Xzerop ,NFFT))./BTM;
LPC=1;
while LPC <= MAXIT
    %First Step*********
    for H=1:ColumnX
        for Q=1:NFFT
            if abs(fftXzerop(Q,H)) > UPLM(Q,1)
                ZXM(Q,H)=(UPLM(Q,1)).*fftXzerop(Q,H)/abs(fftXzerop(Q,H));
            elseif abs(fftXzerop(Q,H)) < LOWLM(Q,1)
                ZXM(Q,H)=(LOWLM(Q,1).*fftXzerop(Q,H))/abs(fftXzerop(Q,H));
            else
                ZXM(Q,H)=fftXzerop(Q,H);
            end
        end
    end


    for P=1:ColumnX
        BTM(:,P)=BTM(1,P)*(ZXM(:,P))'*fftXzerop(:,P)/(ZXM(:,P)'*ZXM(:,P));
    end
    VMAT=zeros(NFFT,ColumnX);
    for K=1:ColumnX
        VMAT(:,K)=AFT*ifft(BTM(1,K)*ZXM(:,K),NFFT);
    end
    intM=exp(1i*angle(VMAT(1:RowX,:))).*Window;
    XPA2=[intM ; zeros(NFFT-RowX,ColumnX)];
    fftXzerop=AFT*(fft(XPA2,NFFT))./BTM;
    LPC=LPC+1;
end
outS=XPA2(1:RowX,:);
```

```
BP=BTM;
end
```